

# Lawrence Berkeley National Laboratory

## Recent Work

### Title

Techno-economic analysis and life-cycle greenhouse gas mitigation cost of five routes to bio-jet fuel blendstocks

### Permalink

<https://escholarship.org/uc/item/13p8z1db>

### Journal

Energy and Environmental Science, 12(3)

### ISSN

1754-5692

### Authors

Baral, NR  
Kavvada, O  
Mendez-Perez, D  
[et al.](#)

### Publication Date

2019-03-01

### DOI

10.1039/c8ee03266a

Peer reviewed

## Techno-economic analysis and life-cycle greenhouse gas mitigation cost of five routes to bio-jet fuel blendstocks

Nawa Raj Baral<sup>a,b</sup>, Olga Kavvada<sup>a,c</sup>, Daniel Mendez Perez<sup>a,b</sup>, Aindrila Mukhopadhyay<sup>a,b</sup>, Taek Soon Lee<sup>a,b</sup>, Blake A. Simmons<sup>a,b</sup>, Corinne D. Scown<sup>\*a,b,c</sup>

Received 00th January 20xx,  
Accepted 00th January 20xx

DOI: 10.1039/x0xx00000x  
[www.rsc.org/](http://www.rsc.org/)

Decarbonizing the air transportation sector remains one of the most challenging hurdles to mitigating climate change. Lignocellulosic biomass-derived jet fuel blendstocks can contribute to the shift toward renewable, low-carbon energy sources for aircrafts. Producing these renewable jet fuel molecules from biomass requires advanced pathways with the potential for efficient and affordable conversion routes. This paper presents a detailed techno-economic analysis and sensitivity analysis, including estimated minimum selling price (MSP), and life-cycle greenhouse gas (GHG) mitigation costs for five routes to four potential bio-jet fuel molecules – limonane via limonene, limonane via 1,8-cineole, tetrahydromethylcyclopentadiene dimer (RJ-4), bisabolane, and epi-isozizaane. The simulated biorefineries utilize biomass sorghum and an integrated high-gravity ionic liquid-based biomass deconstruction process. We present results reflecting the current state of the technology and potential future scenarios with improved yields. Among the conversion pathways and the fuel molecules evaluated in this study, limonane, bisabolane, and epi-isozizaane could reach an MSP of \$0.73- \$0.91 per L-Jet A (\$2.75-\$3.45 per gal-Jet A) in optimized future cases, without a hypothetical lignin-derived co-product. RJ-4 requires a more costly upgrading process and catalysts, resulting in a comparatively higher MSP (\$1.33/L-Jet A or \$5.04/gal-Jet A). Based on the GHG footprints of each fuel, the minimum achievable carbon mitigation cost relative to conventional Jet-A is \$29/metric ton CO<sub>2e</sub>, which is just under double the current cap-and-trade market price in California. Absent any policy supports, the economics could be improved through high-value uses for lignin. To reach a target selling price of \$0.66/L-Jet A (\$2.50/gal), lignin-derived products would need to be sold for at least \$1.9/kg. However, the higher energy density of these bio-based blendstocks offers valuable improvements in aircraft efficiency/range; we find that commercial airlines may be willing to pay a 4-14 cent/L premium for these bio-jet fuels. Our results highlight the need for improvements beyond currently-reported yields for the biologically-produced intermediates, identification of ideal microbial hosts, selection of metabolic pathways to achieve competitive production costs, and a focus on fuels with attractive properties that increase their value.

### Broader context

Given international commitments to reducing greenhouse gas emissions, technological challenges in decarbonizing the aviation sector, and incompatibility of ethanol in current jet engines, there is interest in producing renewable jet fuel molecules (C8-C16) from lignocellulosic biomass. Biologically-produced jet fuel molecules are in early stages of development relative to more mature thermochemical routes. An advantage of biological routes is their ability to produce naphthenes (approximately one third of jet fuel), whereas most other alternative jet fuel processes produce paraffins. Gauging the long-term potential for biological routes requires evaluation of both the current and potential future state of the conversion technologies. This study employs techno-economic analysis to compare five routes to four bio-jet fuel molecules, including a robust sensitivity analysis, to identify cost drivers, bottlenecks, and opportunities for optimization and process intensification. The results highlight a subset of the original five routes that could reach competitive prices, and the premium airlines may be willing to pay for more energy-dense fuels. However, these routes still require a relatively high-value lignin-derived co-product or a modest price for carbon mitigation to compete with Jet-A. This study lays the groundwork for evaluating the long-term competitiveness of bio-based jet fuel production routes and establishing performance targets

<sup>a</sup> Joint BioEnergy Institute, Lawrence Berkeley National Laboratory, Berkeley, California 94720, United States

<sup>b</sup> Biological Systems and Engineering Division, Lawrence Berkeley National Laboratory, Berkeley, California 94720, United States

<sup>c</sup> Energy Analysis and Environmental Impacts Division, Lawrence Berkeley National Laboratory, Berkeley, California 94720, United States.

\*Corresponding author, E-mail: [cdscown@lbl.gov](mailto:cdscown@lbl.gov)

†Electronic Supplementary Information (ESI) available: [Input data for process modeling and detailed probabilistic cost and emissions results for each production step]. See DOI: 10.1039/x0xx00000x

## 1. Introduction

Petroleum-derived jet fuel consumption in the United States (U.S.) was 93.9 billion liters in 2016, representing about 30% of global jet fuel consumption.<sup>1</sup> The aviation sector is responsible for a growing share of global greenhouse gas (GHG) emissions; currently at 2%, and projected to reach 5% by 2050.<sup>2,3</sup> In the U.S., jet fuel accounts for 9% of the total GHG emissions associated with transportation sector.<sup>4</sup> Biological routes for converting lignocellulosic biomass to fuels offer the advantage of producing single-molecule blendstocks, with consistent composition and specifications, that can be drop-in replacements for current jet fuel components. Jet fuel derived from biomass also offers potentially substantial GHG emission reductions,<sup>3</sup> a reduced reliance on petroleum, and the potential to increase domestic energy production in countries with sufficient biomass resources. Additionally, while progress has been made in the decarbonization of ground transportation,<sup>5</sup> complete decarbonization of the aviation sector remains challenging with current technologies.<sup>6</sup> In the near-term, there is still a compelling need to produce renewable replacements for cycloparaffinins, aromatics, as well as straight-chain and branched alkanes (C8-C16)<sup>7</sup> that lend jet fuel its higher energy density, and flow and combustion characteristics. In this paper, we provide the first detailed techno-economic analysis (TEA) for five routes to producing four promising jet fuel molecules from lignocellulosic biomass via biological routes. We compare the economics of production, the cost of GHG mitigation relative to conventional aviation fuel, impacts of increased energy density on air travel economics and efficiency, and recommend potential improvements given the state of technology.

Monoterpenes (C10 isoprenoids), such as limonene, 1,8-cineole, and linalool are promising potential precursors for jet fuel<sup>8–10</sup> due to their low freezing point and high energy density. A recent study<sup>9</sup> investigated properties of jet fuel and several hydrocarbons such as n-butanol, n-hexanol, butyl levulinate, butyl butyrate, ethyl octanoate, methyl linolenate, farnesene, ethyl cyclohexane, and limonene. Among these hydrocarbon fuels, Chuck and Donnelly reported that limonene could be an excellent substitute for jet fuel based on its properties.<sup>9</sup> However, direct combustion of alkenes (such as limonene) can negatively impact engine performance due to the formation of gums.<sup>11</sup> In addition to monoterpenes, sesquiterpenes (C15 isoprenoids), such as bisabolene and epi-isozizaene are other potential jet fuel precursors.<sup>12–14</sup> These mono- and sesquiterpenes can be transformed into their saturated forms (alkanes) through either hydrogenation or oligomerization and hydrogenation, which is required before blending into jet fuel (Fig. 1). Hereafter, we focus on limonane (via two different biologically-produced intermediates, limonene and 1,8-cineole), RJ-4, bisabolane, and epi-isozizaane (Fig. 1).

Even at near-theoretical fuel yields, sustainable feedstock supplies, deconstructed to cheap fermentable sugars, are prerequisites to achieving commercially-viable production

of isoprenoids. In this paper, we simulate different jet fuel routes in the context of biorefineries utilizing a biomass sorghum feedstock and an integrated high-gravity ionic liquid (IL) deconstruction process. Further background on sorghum feedstocks and IL deconstruction processes can be found in the Electronic Supplementary Information (ESI)-S1.1. After liberating fermentable sugars at high yields, the next challenge is the development of efficient microbial conversion pathways to produce the desired isoprenoids.

There are two major natural biosynthetic pathways to produce isoprenoids: (i) mevalonate-dependent isoprenoid pathway (MVA pathway) for eukaryotes (except some plants and some bacteria) and the mevalonate-independent 1-deoxy-D-xylulose-5-phosphate pathway (DXP pathway) for most prokaryotes.<sup>10,15</sup> These pathways have been engineered in two host microorganisms, *Saccharomyces cerevisiae* and *Escherichia coli*, to increase biofuel yield and titer, increase sugar loading levels, and reduce the cytotoxicity of the targeted biofuel.<sup>10,15</sup> For instance, tolerance mechanisms, such as efflux pumps that export toxins from the cell using the proton motive force, reduce the toxicity from limonene accumulation and improves yield.<sup>8</sup> Additionally, *E. coli* is a promising host due to its potential to utilize a wide range of sugars (both glucose and xylose) under aerobic (aeration rate of 1-2 volume of air per volume of liquid solution per minute, referred to as vvm)<sup>10,16,17</sup> and microaerobic conditions (aeration rate of 0.2-0.6 vvm).<sup>16–19</sup> Other benefits of using *E. coli* are easier gene regulation and expression, wealth of genetic tools available for metabolic and host engineering, rapid growth, and suitability for a variety of industrial products.<sup>20,21</sup> The aerobic and microaerobic pathways require more operating energy for reactor cooling and air supply relative to anaerobic fermentation, but reduce bioconversion time and increase product yield.<sup>22,23</sup> These trade-offs present an interesting opportunity to optimize on the basis of energy requirements, production costs, and GHG emissions.

No previous studies have provided a detailed TEA and estimated the GHG mitigation costs for the biological production of these isoprenoids. Through rigorous process simulation, stochastic uncertainty analysis, and scenario analysis, this paper highlights the challenges faced in developing cost-competitive biologically-produced isoprenoid aviation fuel blendstocks and long-term potential. Because lignin valorization is a focus of intense interest in the bioenergy research community, and provides an opportunity to improve biorefinery economics, this paper also presents the required selling price of lignin-derived products to reach the targeted selling price of \$0.66/L (\$2.50/gal) of bio-jet fuel, assuming lignin conversion costs similar to those of pyrolysis. TEA at this early stage in scientific research and technology development is vital to elucidating the long-term potential for achieving cost parity with conventional fuels, the relative GHG mitigation costs, process bottlenecks, and research strategies most likely to improve performance.

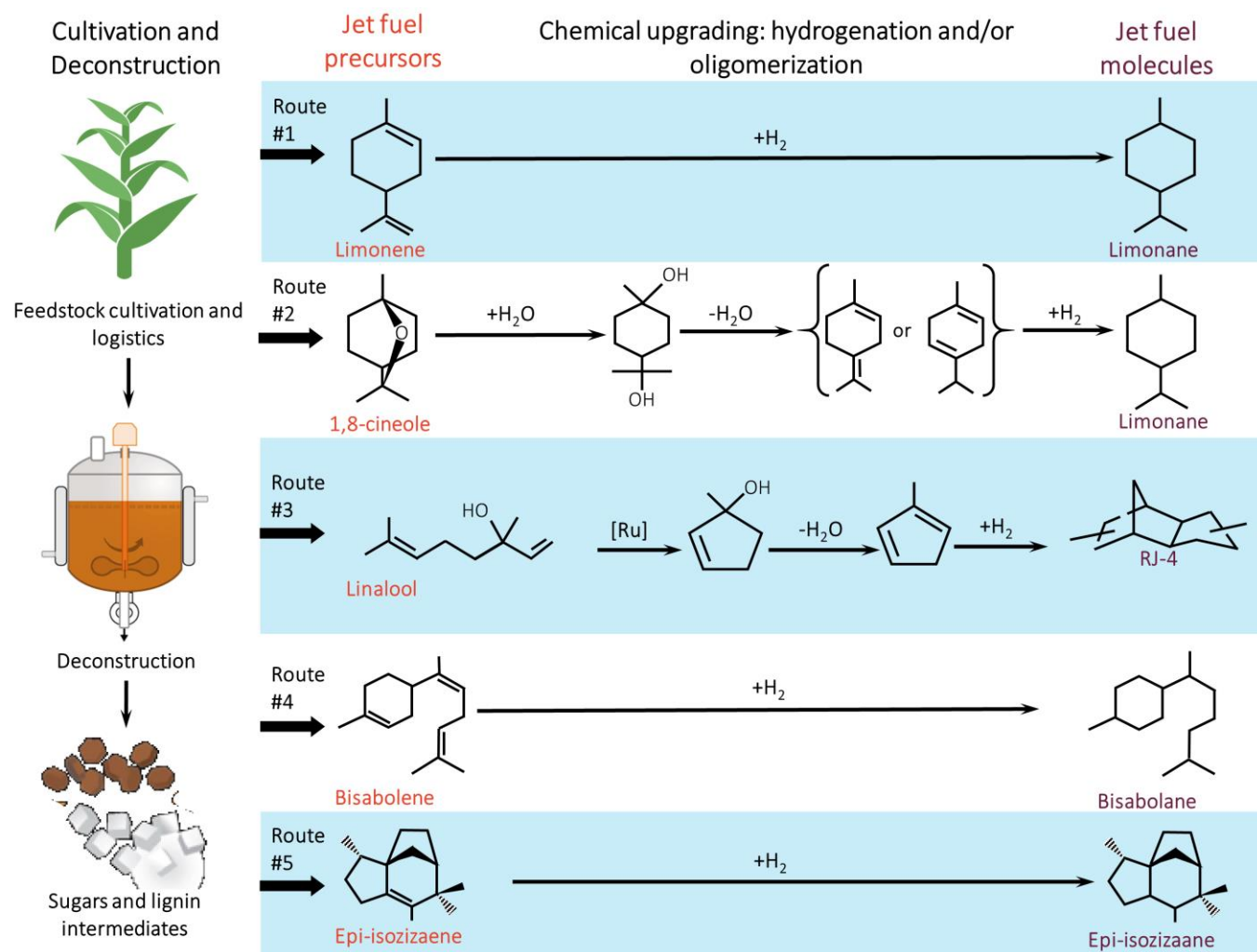


Fig. 1. A visual representation of how the five jet fuel molecules studied are produced from biomass-derived sugars and their respective conversion pathways. Upstream processes of each route (routes #1-5) include lignocellulosic biomass feedstock supply logistics, ionic liquid pretreatment, simultaneous saccharification and bioconversion by using *E. coli*, and recovery and separation of the jet fuel precursor. The upgrading process was developed considering previous studies/ U.S. Patent on limonene;<sup>11</sup> 1,8-cineole;<sup>24</sup> linalool;<sup>25</sup> bisabolene;<sup>26,27</sup> and epi-isozizaene<sup>28</sup> although these jet fuel precursors are still in the research phase. Limonene, bisabolene, and epi-isozizaene require only hydrotreating. 1,8-cineole requires ring-opening, dehydration, and hydrogenation steps.<sup>24</sup> Linalool requires dehydration, dimerization, hydrogenation, and isomerization processes.<sup>25</sup>

## 2. Methods

### 2.1 System overview

The aim of this study is to quantify and compare the minimum selling price and GHG emissions mitigation costs for five promising bio-jet fuel production pathways. Fig. 2 depicts the system boundaries for this study. The analysis includes feedstock supply logistics, feedstock handling and pre-processing, IL pretreatment, simultaneous saccharification and bioconversion, recovery and separation of the IL and jet fuel precursor, precursor upgrading (hydrogenation or oligomerization plus hydrogenation), wastewater treatment, and on-site energy generation. Our system boundary ends at the biorefinery gate, although we do include a separate additional analysis of possible differences in aircraft efficiency and per-passenger costs resulting from increased fuel energy density. The following sections discuss the process modeling methods, data sources, and assumptions made in this study.

Unless otherwise specified, the process models use assumptions consistent with the feedstock supply logistics analyses conducted by Idaho National Laboratory (INL)<sup>29,30</sup> and Oak Ridge National Laboratory (ORNL),<sup>31-33</sup> the downstream conversion process developed by National Renewable Energy Laboratory (NREL),<sup>34-36</sup> and similar previous studies<sup>37-39</sup> conducted at the DOE Joint BioEnergy Institute (JBEI). All dollar values are reported in 2018 U.S. dollars.

**2.1.1 Feedstock supply and handling.** Biomass sorghum serves as the sole feedstock in this analysis, based on an average composition of different biomass sorghum varieties. The simulated biorefinery utilizes dry biomass at 1814 metric tons (t)/day (2000 dry ton/day). The high-yielding sorghum feedstock can be collected within a supply radius of <80 km if the land utilization for biomass feedstock is at least 2% of the total land and dry matter loss over the biomass supply chain is 20 wt% or less.<sup>40</sup> Under these conditions, a recent study by Baral

et al.<sup>41</sup> found that direct transportation of biomass from field to the biorefinery is more cost-effective strategy than any depot/densification model. The delivered feedstock cost includes nutrient replacement, silage harvesting, infield transportation, collection at the field edge, transportation to the biorefinery, and outdoor storage next to the biorefinery. The average composition of sorghum biomass is calculated based on several previous studies.<sup>42–49</sup> The full list of costs and assumptions is provided in the ESI-S1.1 and S2. The result is an average delivered cost of \$86.15/t (dry) sorghum, with a range of \$60–120/t-dry. The feedstock handling process at the biorefinery is consistent with NREL's feedstock handling/processing model,<sup>34,35</sup> which is summarized in the ESI-S1.2.

**2.1.2 Pretreatment.** The preprocessed (milled) biomass is mixed with water and IL, and delivered to the pretreatment reactor. Biomass feedstock and IL loading rates are maintained at 30 wt%, and 0.29 kg/kg-total solids (about 10 wt% in the total

slurry), respectively.<sup>34,37,38</sup> The baseline model was developed with cholinium lysinate ([Ch][Lys]) due to its high glucose and xylose yields (about 90 wt%) during enzymatic hydrolysis, and an additional case was developed based on a promising protic IL -- ethanolamine acetate ([EOA][OAc]).<sup>37–39</sup> [Ch][Lys] is a basic IL and requires acid<sup>39</sup> to adjust the pH before hydrolysis and bioconversion, while [EOA][OAc] does not. Table 1 summarizes the operating parameters associated with the IL pretreatment process. The possible ranges for these input parameters and their probability distributions are summarized in ESI-Table S2. A more detailed discussion on the selected ILs and their operating parameters is available in previous literature.<sup>37–39</sup> A heat exchanger recovers 80% of the maximum recoverable heat from the slurry exiting the pretreatment slurry. Centrifugal pumps were used to handle biomass slurries and process chemicals. Following the pretreatment process, the pretreated slurry undergoes simultaneous saccharification and bioconversion with or without pH adjustment, depending on the IL choice discussed above.

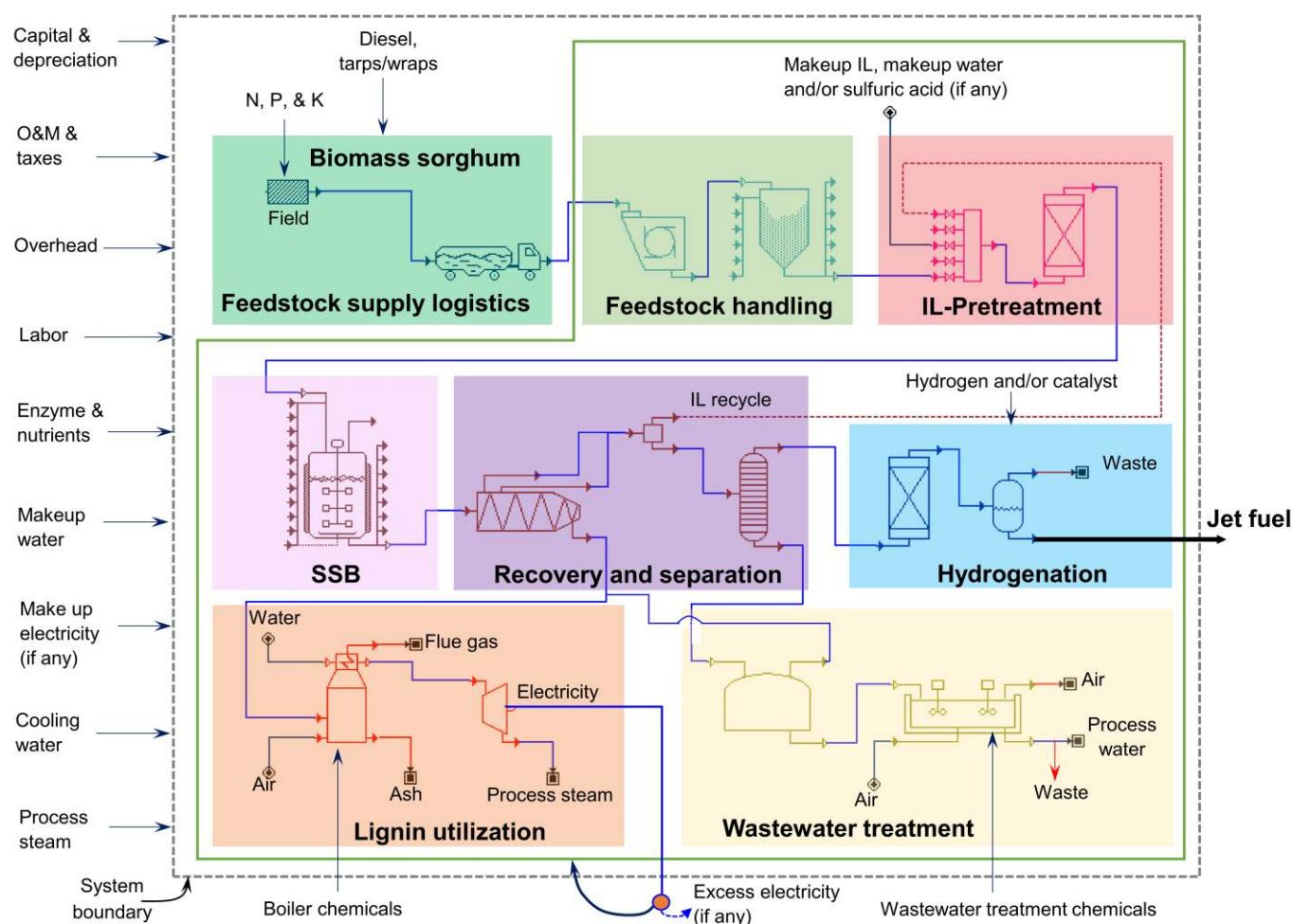


**Fig. 2** System boundary for TEA with major jet fuel production stages, and selected process equipment with cost, energy, and material inputs (N: nitrogen, P: phosphorous, K: potassium, SSB: simultaneous saccharification and bioconversion).

Table 1. Major operating and process parameters used to develop process model and determine the required material, energy and cost<sup>a</sup>

Process parameters	Units	Baseline <sup>φ</sup>	Optimal <sup>λ</sup>	Process parameters	Units	Baseline <sup>φ</sup>	Optimal <sup>λ</sup>
<b>Feedstock composition</b>				Glucose conversion	wt%	17.5	29.2
Cellulose <sup>42–49</sup>	wt%	35.8	40	Xylose conversion	wt%	17.5	29.2
Hemicellulose <sup>42–49</sup>	wt%	22.9	27.4	<i>1,8-cineole</i> <sup>10,6</sup>			
<b>IL Pretreatment</b>				Bioconversion time	h	48	36
Solids loading rate <sup>34,37,38</sup>	wt%	30	30	Glucose conversion	wt%	18.3	33.0
IL-loading rate <sup>37</sup>	kg/kg-dry biomass	0.29	0.29	Xylose conversion	wt%	18.3	33.0
IL-cost <sup>37,39</sup>	\$/kg	2	1	<i>Linalool</i> <sup>10</sup>			
Sulfuric acid loading <sup>37,39</sup>	kg-acid/kg-IL	0.2	0	Bioconversion time	h	48	36
Sulfuric acid price <sup>34–36</sup>	\$/kg	0.14	N/A	Glucose conversion	wt%	18.3	33.0
Lignin to soluble lignin	wt%	65	65	Xylose conversion	wt%	18.3	33.0
Pretreatment time	h	3	3	<i>Bisabolene</i> <sup>50</sup>			
<b>Enzymatic hydrolysis</b>				Bioconversion time	h	72	36
Solid loading rate	wt%	20	30	Glucose conversion	wt%	17.5	29.2
Enzyme loading rate	mg/g glucan	20	7	Xylose conversion	wt%	17.5	29.2
Cellulose to glucose with [Ch][Lys]	wt%	84	N/A	<i>Epi-isozaena</i> <sup>6</sup>			
Xylan to xylose with [Ch][Lys]	wt%	80	N/A	Bioconversion time	h	72	36
Cellulose to glucose with Protic IL	wt%	80	95	Glucose conversion	wt%	17.5	29.2
Xylan to xylose with Protic IL	wt%	75	90	Xylose conversion	wt%	17.5	29.2
Hydrolysis time	h	72	72	<b>Recovery and separation</b>			
Enzyme price	\$/kg-protein	5	5	Recovery of the jet fuel precursor (assumed <sup>34</sup> )	wt%	97	97
<b>Bioconversion</b>				IL-recovery <sup>37,38,51</sup>	wt%	97.5	99
Cost of corn steep liquor <sup>34–36</sup>	\$/kg	0.1	0.1	<b>Hydrogenation and oligomerization</b>			
Cost of DAP <sup>34–36</sup>	\$/kg	1	1	Hydrogen loading rates <sup>β</sup>	wt%	β	β
<b>Aerobic Pathways</b>				Hydrogen cost <sup>36</sup>	\$/kg	1.5	1.5
Aeration rate <sup>10,16,17</sup>	VVM	1	N/A	Ru (catalyst) cost <sup>52</sup>	\$/kg	253.5	253.5
Power consumption <sup>53</sup>	kW/m <sup>3</sup>	3	N/A	Dehydrating catalyst cost <sup>54</sup>	\$/kg	1.12	1.12
Power dissipation to heat <sup>22,53</sup>	%	80	N/A	Hydrogenation catalyst (Pd/Ac) cost <sup>52,54</sup>	\$/kg	276.3	276.3
<b>Micro-aerobic pathways</b>				Oligomerization catalyst (AlCl <sub>3</sub> ) cost <sup>54</sup>	\$/kg	284.4	284.4
Aeration rate <sup>16–19</sup>	VVM	0.35	0.2	*Cyclohexane <sup>55</sup>	\$/kg	0.39	0.39
Power consumption <sup>53</sup>	kW/m <sup>3</sup>	0.5	0.1	<b>Lignin utilization</b>			
Power dissipation to heat <sup>22,53</sup>	%	40	30	Boiler chemicals price	\$/kg	5	5
<b>Limonene</b> <sup>50</sup>				Natural gas price	\$/kg	0.2	N/A
Bioconversion time	h	72	36				

**Yield Scenarios:** Current Yield (CY) – Baseline values with current best-reported product yield, Baseline Yield (BY) – Baseline values with 50% of stoichiometric theoretical yield, Theoretical Yield (TY) – Baseline values with 100% of stoichiometric theoretical yield

<sup>φ</sup> The yields of different jet fuel precursors from glucose and xylose under the “Baseline” column refer to the baseline yield (BY), which is 50% of their stoichiometric theoretical yields (Table 2 and ESI-Figure S3)

<sup>λ</sup> The “Optimal” scenario considers a micro-aerobic bioconversion pathway, protic IL-based biomass deconstruction, product yield of 90% of the stoichiometric theoretical yield, and other optimal process parameters listed under the “optimal” column.

<sup>a</sup> Unless otherwise specified data summarized in this table were gathered from recent studies.<sup>37–39</sup>

<sup>δ</sup> Based on recent unpublished experimental results from JBEI/LBNL.

<sup>β</sup> Estimated mass of hydrogen loading rates (g/100-g of precursor) for limonene, 1,8-cineole, linalool, bisabolene, and epi-isozezaene are 3.5, 1.5, 1.5, 3.5, and 1.2, respectively.

\*Yang et al.<sup>24</sup> demonstrate a faster hydrogenation process of 1,8-cineole with addition of cyclohexane. Therefore, cyclohexane is considered only for the hydrogenation process of 1,8-cineole.

**2.1.3 Simultaneous saccharification and bioconversion.** The ILs modeled in this study disrupt the structure of biomass by dissolving out 60% of the lignin fraction of biomass<sup>37,38</sup> to increase the accessible surface area for the enzyme. The enzyme then transforms most of the cellulose and hemicellulose into fermentable sugars (primarily glucose and xylose) during enzymatic hydrolysis (Table 1 and ESI-Table S2). These sugars are simultaneously metabolized by *E. coli* to

produce individual jet fuel precursors from the set of molecules defined previously: limonene, 1,8-cineole, linalool, bisabolene, and epi-isozizaene. For the baseline scenario, cellulase enzymes are used at a loading rate of 20 mg protein per gram cellulose.<sup>34</sup> The total solids loading rate for this process is maintained at 20 wt% by supplying additional water.<sup>34</sup> In addition to the enzyme, inoculum from the seed train is fed at 10 vol% along with the nutrient nutrients: corn steep liquor (CSL) at 0.25 wt% and diammonium phosphate (DAP) at 0.33 g/L-whole slurry.<sup>34</sup> *E. coli* metabolizes the fermentable sugars under aerobic conditions in the baseline analysis. Table 1 and ESI-Table S2 summarize all the operating conditions and conversion rates used for analysis in this study. Following the bioconversion, a mixture of jet fuel precursor and stillage (process chemicals, water, and unutilized materials) are delivered to the recovery and separation unit.

**2.1.4 Recovery and separation.** In addition to the product, recovery of the IL is very important to reduce costs associated with makeup IL (IL costs about 18-fold more than sulfuric acid).<sup>34,37,38</sup> In this section, centrifugation followed by ultrafiltration separates most of the solid fraction of the product slurry. Our baseline analysis assumes a 97% IL recovery rate, and 50% recovery of water available in the input stream after the successive pervaporation process. In the case of [Ch][Lys], a pH adjustment step is required prior to hydrolysis and an additional 'regeneration' step is required prior to recycling the recovered IL. This can be accomplished by an electrodialysis system, as discussed in more detail in previous literature.<sup>56,57</sup>

Following IL recovery, the jet fuel precursor is recovered through multiple distillations and a decantation system. The boiling points of all the jet fuel precursors considered in this study are above 175°C, thus, the first distillation column separates the remaining water, jet fuel precursor, and other volatile compounds (such as acetic acid) from the remaining solids and other materials. Subsequent decantation removes most of the water and volatile compounds. A second distillation column purifies the jet fuel precursor by removing the remaining water and other compounds. Following this recovery, about 99.5 wt% pure jet fuel precursor is delivered to the upgrading process (Fig. 1). Alternatively, both capital and operating costs of distillation can be slightly reduced if the decanter is used before the distillation. This is highly dependent on the fraction of the water that can be separated in the decanter with the minimal loss of the fuel precursor. To date, there is not sufficient experimental data for the recovery and separation processes to confidently identify the best configuration. This study uses an assumed 5% loss rate during recovery and separation of the fuel precursor. Water and other volatile compounds are delivered to the wastewater treatment unit and the solid fraction from the centrifugation and ultrafiltration process is delivered to the lignin utilization unit.

**2.1.5 Oligomerization and hydrogenation.** Saturated hydrocarbons (alkanes) are the basis of petroleum fuels.<sup>11</sup> All the jet fuel precursors considered in this study are alkenes. Direct utilization of these alkenes could form gums during combustion.<sup>11</sup> To ensure compatibility with jet engines, limonene, bisabolene, and epi-isozizaene are transformed into their respective alkanes through hydrogenation (Fig. 1). However, 1,8-cineole and linalool require more extensive upgrading. 1,8-cineole requires ring-opening, dehydration, and

hydrogenation steps in its conversion to limonane.<sup>24</sup> Linalool requires dehydration, dimerization, hydrogenation, and isomerization processes to produce RJ-4 (Fig. 1).<sup>25</sup> Previous studies on limonene,<sup>11</sup> 1,8-cineole,<sup>58</sup> linalool<sup>54,59,60</sup> bisabolene,<sup>12–14</sup> and epi-isozizaene<sup>28,61</sup> provide additional information about these molecules and the upgrading process.

#### 2.1.6 Wastewater treatment and on-site energy generation.

Both wastewater and on-site energy generation sections are consistent with the NREL model.<sup>34</sup> Wastewater was assumed to be treated through anaerobic digestion followed by aerobic treatments. All the process conditions and data are consistent with the NREL study<sup>34</sup> and other recent works<sup>37,38</sup> as summarized in ESI-Table S2. The on-site energy generation unit is comprised of two major pieces of capital equipment: (i) the boiler to generate steam by utilizing lignin, biogas, makeup natural gas, and other unutilized cellulose and hemicellulose fractions; and (ii) the steam turbine to generate electricity. Electricity and exhaust steam from the turbine are supplied to upstream processes. Excess electricity (if any) can be exported to the grid, resulting in an economic and emissions credit. Air required for the boiler is delivered through the air compressor.

#### 2.2 Techno-economic analysis

As discussed earlier, the simulated biorefinery utilizes dry lignocellulosic biomass feedstock at a rate of 1814.4 t/day (2000 short tons/day). ESI-Table S2 summarizes compositions of biomass sorghum used in this study. The techno-economic model for jet fuel production from sorghum biomass feedstock was developed by using a modeling software SuperPro Designer (SPD) v10.<sup>55</sup> The SuperPro TEA model was integrated with Microsoft Excel by using Visual Basic Programming to plug in input data and extract the required results including capital and operating costs, jet fuel production cost, materials, process energy, and direct emission. All the capital and operating data extracted from SPD are used to determine the minimum selling price by using Microsoft Excel as SPD only provides the production cost excluding income tax and internal rate of return (IRR). The TEA model developed in SPD encompasses all the required processes as discussed earlier (method sections 2.1.2–2.1.6). After completing the process model, a material and energy balance analysis followed by economic analysis were conducted by using SPD's built-in mass and energy balance tool. The material and energy balance data were used to determine the required size of equipment and respective purchasing price, the capital investment, and operating costs. Equipment purchase prices are assigned using  $n^{\text{th}}$  plant assumptions, exponential scaling, price index adjustments as detailed in the NREL report.<sup>34</sup> A built-in mathematical function in SPD adjusts the equipment purchase price based on the required size of process equipment and the analysis year (2018). Installation factors gathered from the NREL report<sup>34</sup> are then assigned to each piece of process equipment to determine the installed cost. Other direct and indirect cost parameters were assigned based on the method discussed in the previous study conducted by NREL<sup>34</sup> to determine total direct fixed capital (DFC). Then, the total capital investment (TCI) was estimated by incorporating DFC, working capital, and start-up costs. An operating cost of one month was assigned as working capital and 5% of the total DFC was assigned for start-up cost.



In addition to capital investment, the annual operating cost was estimated by incorporating facility-dependent cost (includes maintenance (1% of DFC), depreciation (decline balance method<sup>34</sup>), and property taxes and insurance (0.7% of DFC), raw materials cost, labor-dependent cost and cost of utilities. Operator cost of \$52.67/h<sup>55</sup> was assigned in the SPD model, which includes the basic rate of \$22.9/h, and the sum of benefits, operating supplies, supervision, and administration factor of 0.4, 0.1, 0.2 and 0.6 times of the basic rate, respectively. While the required process steam is generated from the on-site energy generation section, the cost of the cooling water and chilled water of \$0.05/t and \$0.4/t, respectively, were assigned in the SPD model.<sup>55</sup> After assigning all the capital and operating costs, the minimum selling price of jet fuel was estimated considering annual operating hours of biorefinery of 7920 h (330 days/year and 24 hours/day) for 30 years. Consistent with the NREL study,<sup>34</sup> we use an IRR of 10%. Additionally, any excess electricity generated through lignin utilization was assigned as a credit with the selling price of 0.07 \$/kWh assuming the industrial application.<sup>62</sup> This is a conservative estimate relative to the feed-in tariffs offered to bioenergy projects in programs such as Pacific Gas & Electric's BioMAT program (\$0.128/kWh).<sup>63</sup>

### 2.3 Life-cycle GHG mitigation cost

In addition to TEA, we calculated the life-cycle GHG mitigation cost considering the MSP of bio-derived jet fuel relative to Jet-A and the net GHG emissions difference when bio-jet fuel replaces the equivalent quantity of petroleum-based jet fuel. A life-cycle GHG footprint of 89 gCO<sub>2e</sub>/MJ<sup>64</sup> was used for petroleum-derived jet fuel. More details on calculating GHG mitigation costs are available in previous literature.<sup>65,66</sup> The life-cycle GHG emissions associated with the production of our selected jet fuel molecules are documented in our previous study.<sup>67</sup> Additional methods and assumptions used to estimate the GHG emissions are discussed in ESI-S1.3.

### 2.4 Scenario analysis

In addition to the baseline scenario, two main alternative scenarios were investigated in this study to identify a most cost-effective and sustainable jet fuel production route. These scenarios are discussed in the following section and summarized in Table 2.

**2.4.1 Protic IL pretreatment.** Previous studies conducted at JBEI<sup>38</sup> and elsewhere<sup>51,68</sup> reported that protic ILs could be a potential option to reduce overall costs with sugar yields of above 80% of theoretical. Ease of recovery is the most important factor, as protic ILs do not require pH adjustment before hydrolysis and bioconversion, thus avoiding a regeneration step as discussed earlier for [Ch][Lys]. However, the sugar yield with currently-demonstrated protic IL is still lower than [Ch][Lys]. Additionally, protic IL cost could be around \$1/kg, compared to \$2/kg assumed in our Baseline scenario.<sup>51,68</sup> This study presents both the minimum selling price and GHG emissions comparisons with [Ch][Lys] and [EOA][OAc] by considering the above trade-off between these two ILs.

**2.4.2 Bioconversion pathways and product yields.** *E. coli*, the microorganism considered in this study for the production of jet fuels, being a facultative anaerobe does not require oxygen to grow but grows better in the presence of oxygen. Generally, *E.*

*coli* strains metabolize five and six carbon sugars at a faster rate under aerobic condition when compared to their sugar utilization rate under anaerobic conditions.<sup>20,23</sup> However, degradation of aromatics by this organism requires O<sub>2</sub> as an electron acceptor and a co-substrate. Thus, completely anaerobic conditions are not feasible for producing jet fuel molecules considered in this study by using *E. coli* strain(s) due to low yield/titer. However, it is possible for this organism to ultimately produce isoprenoids under micro-aerobic conditions, with additional research efforts. Micro-aerobic conditions reduce the energy required to supply air, agitation energy, and chilled water required to maintain a constant operating temperature (37 °C) in the reactor. Thus, micro-aerobic conditions were considered in this study to illustrate the potential benefits of reducing oxygen requirements.

Table 2. Different Scenarios considered in this study for each of the selected renewable jet fuel blendstock.

Bioconversion aeration	Ionic liquid	Product yield	Scenario name/ results
Aerobic	[Ch][Lys]-based	Current (CY)	<b>Baseline-CY (Fig. 3)</b>
		50%	
		theoretical (BY)	<b>Baseline-BY (Fig. 3-6)</b>
	[EOA][OAc] (Protic IL)-based	100%	
		theoretical (TY)	<b>Baseline-TY (Fig. 3)</b>
		Current (CY)	See ESI, Fig. S3-4
Microaerobic	[Ch][Lys]-based	50%	
		theoretical (BY)	See ESI, Fig. S3-4
		100%	
	[EOA][OAc] (Protic IL)-based	theoretical (TY)	See ESI, Fig. S3-4
		Current (CY)	See ESI, Fig. S3-4
		50%	
[EOA][OAc] (Protic IL)-based	theoretical (BY)	See ESI, Fig. S3-4	
	90%		
	theoretical (Optimal)	<b>Optimal (Fig. 7-8)</b>	
	100%		
		theoretical (TY)	See ESI, Fig. S3-4

Note: Yield values are based on the current best-reported product yield (Current) or as a percentage of stoichiometric theoretical yield. Scenarios bolded are included in main text, while those not documented in main text are listed with the results location in the ESI. More process parameter details are included in Table 1.

In addition to bioconversion pathways, jet fuel production cost and GHG emissions were also estimated using different product



yields, including the best currently-reported yield, baseline yield (assumes 50% of the maximum theoretical yield), and stoichiometric maximum theoretical yield (estimated by using stoichiometric chemical equation and glucose and xylose without considering biological limitations). The estimated stoichiometric maximum theoretical yields of limonene, 1,8-cineole, linalool, bisabolene and epi-isozizaene are about 32.4, 36.7, 36.7, 32.4, and 32.4 g/100 g-fermentable sugar (glucose and xylose).<sup>8</sup>

### 2.5 Uncertainty analysis and optimal jet fuel cost

Uncertainty associated with jet fuel production costs was assessed by using single point and two-point sensitivity analyses, and by assigning appropriate probability distributions to all the input parameters (ESI-Table S2). Several sets of two most influential parameters identified from the single point sensitivity analysis were considered for two-point sensitivity to determine the impact on the minimum selling price with their concurrent variations. While the single point sensitivity analysis in this study is useful to identify the most influential input parameters to the jet fuel production cost and GHG mitigation

costs, Monte Carlo simulations provide valuable additional insight into the likelihood of achieving specific targets. Standard deviation and the allowable range of input parameters used for analysis in this study are summarized in ESI-Table S2. The minimum and maximum values of each input parameter were used for sensitivity analysis. Input parameters were modeled in the Monte Carlo simulation using four different probability distribution functions: uniform, triangular, normal, and lognormal, to conduct uncertainty analysis. The types of probability distribution were selected based on the variability present in the input parameters. A decision tree for this selection is shown in ESI-S2 (Figure S1). These uncertainty analyses were performed by using SuperPro Designer and the macro-enabled Microsoft Excel based model. The simulation was run for 5000 trials. The macro-enabled Microsoft Excel model developed in this study plugs in the randomly generated input value in the process model developed in SuperPro Designer and exports the required material, cost, and energy results in the Microsoft Excel.

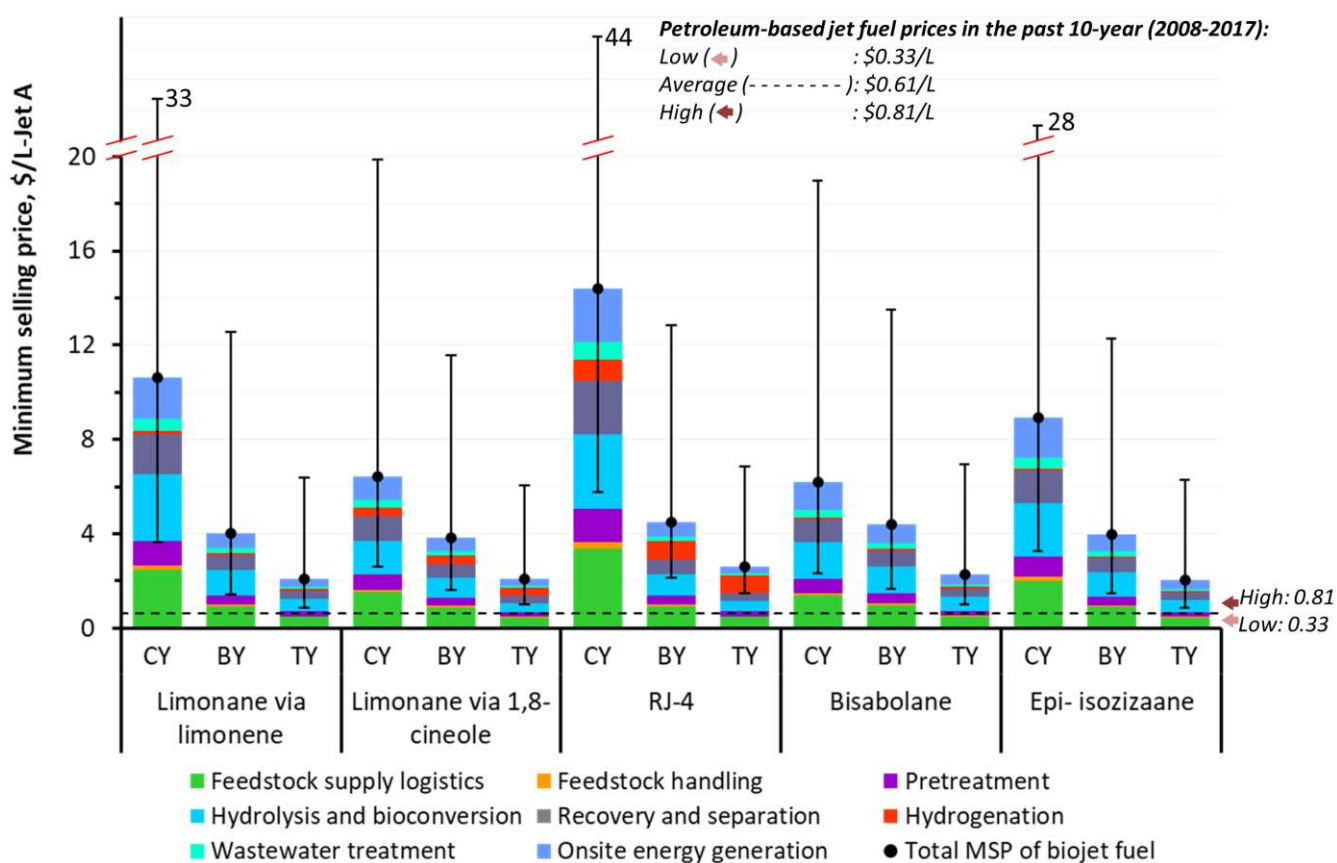


Fig. 3. Minimum selling price of different bio-jet fuel molecules and contribution from different stages of the bio-jet fuel production chain. The sensitivity bars denote optimistic and pessimistic minimum selling price (MSP), based on variations in IL recovery, sugar yield from biomass, biomass feedstock costs, and carbohydrate content in the biomass. CY: Current Yield, BY: Baseline Yield (50% theoretical), TY: Theoretical Yield. These results correspond to [Ch][Lys] pretreatment and aerobic bioconversion. Results for [EOA][OAc] are very similar and are provided in ESI-5. Horizontal dashed line (- - - -) denotes 10-year average jet fuel price at refineries of \$0.61/L.<sup>69</sup> Under the same yield scenarios, switching from aerobic to micro-aerobic bioconversion pathways reduces hydrolysis and bioconversion cost by 30% resulting in 10% lower minimum selling price (ESI-S5). All the bio-jet fuels and petroleum-based jet fuel prices are in 2018 U.S. dollar

### 3. Results and discussion

#### 3.1 Baseline minimum selling prices of jet fuel molecules

For every jet fuel molecule evaluated in this study, hydrolysis and bioconversion, feedstock supply logistics, lignin utilization, recovery and separation, and pretreatment are the major contributors to the minimum selling price. Fig. 3 depicts their total MSPs and relative contributions along with other processing steps of the supply chain from farm to biorefinery gate, using baseline assumption and varying the yield from current to baseline (50% of theoretical) and stoichiometric theoretical maximum. The breakdown between capital and operating costs is provided in the ESI-S4. Regardless of route, feedstock supply and simultaneous hydrolysis and bioconversion are the two largest contributors to cost. The hydrolysis and bioconversion section accounts for 26% of the MSP for limonane via limonene, bisabolane, and epi-isozizaane. This is mainly due to the enzymes and utilities required during hydrolysis and bioconversion, respectively. The utilities can be reduced by decreasing the retention time or switching from aerobic to microaerobic conditions (ESI-S5). The impact of the 33% lower retention time (48 h, summarized in Table 1) can be seen for limonane via 1,8-cineole (Fig. 3), where feedstock cost contributes 23% of the MSP followed by a 21% contribution from hydrolysis and bioconversion. Feedstock supply logistics is also major contributor to other molecules, which account for 20–23% of the bio-jet fuel MSP. Within that category, biomass transportation and nutrient replacement (fertilizer) costs were the major contributors to the biomass feedstock costs, accounting for 40 and 27% of the total biomass feedstock cost at the biorefinery gate, respectively. These costs can be reduced by building the biorefinery in biomass resource-dense areas or engineering for improved yields and nutrient use efficiency. Because aerobic conversion is more energy-intensive than anaerobic fermentation, the lignin fraction of biomass and biogas generated from on-site wastewater treatment process are not sufficient to generate the required electricity and process steam for the biorefinery. We assume that natural gas is used as a supplemental fuel.

In addition to natural gas, the electricity required for water pumping and auxiliary heating to maintain the required temperature of process steam are other major cost components of the on-site energy generation section. The entire on-site energy generation section accounts for 14–19% of the MSP depending on the specific bio-jet fuel molecule, much of which is due to capital expenditures.

The pretreatment section (9–10% of MSP) and recovery and separation section (14–16% of MSP) are also important contributors and, because IL recovery is challenging and costly,

costs in these sections are interrelated. Increasing the solids loading rate and/or reducing or eliminating the required sulfuric acid for pH adjustment before hydrolysis and bioconversion could reduce costs in both sections (ESI-S5). As an alternative to baseline recovery and separation methods of jet fuel precursor (distillation followed by decantation and subsequent distillation), using a decantation process before distillation reduces the system's contribution to the MSP by 1.3–1.5%. Other alternative recovery methods such as membrane-based systems with the operating temperature of <100°C could further reduce recovery and separation costs.

RJ-4 stands out from the other molecules/routes in that the hydrogenation step (including dehydration, hydrogenation, and oligomerization) adds significant cost (17% of MSP). This is primarily due to additional catalyst required for the dehydration and oligomerization step. The downstream hydrogenation process for other jet fuel molecules accounts for 5% of the MSP. Wastewater treatment and on-site feedstock handling are the smallest cost components, accounting for approximately 5% and 2% of the MSP, respectively.

In total, the baseline MSP (including an improvement in yields to reach 50% of stoichiometric theoretical maximum) for our selected bio-jet fuel molecules is still about 7 times greater than the 10-year average U.S. jet fuel selling price at refineries (\$0.61/L).<sup>69</sup> This disparity means that improvements in any individual section will not be sufficient to close the gap. It is worth noting that, although the feedstock and conversion pathways differ, our baseline results are comparable in magnitude to the minimum selling price of jet fuel estimated in previous studies considering: (a) alcohol to jet fuel pathway-\$1.21/L from corn stover<sup>70</sup> and \$1.15–\$4.05/L from wheat straw;<sup>70,71</sup> (b) oil to jet fuel pathway- \$1.23–\$1.43/L from soybean oil<sup>72</sup> and \$3.43–\$9.76/L from algae biomass;<sup>73,74</sup> (c) syngas to jet fuel pathway-\$1.74 from wood chips;<sup>70</sup> and (d) sugar to jet fuel pathways \$1.52/L from corn stover<sup>36</sup> and \$1.21–\$2.19/L<sup>74</sup> from sugarcane. These jet fuel minimum selling prices were normalized by NREL in a previous review.<sup>75</sup> Fig. 4 compares the minimum selling prices of bio-jet fuels included in this study (corresponding to the baseline scenario assumptions) to estimated bio-jet fuel prices from the above-mentioned review<sup>75</sup> and possible future petroleum-derived jet fuel prices (2018\$)<sup>76</sup> based on three crude oil price scenarios. The results indicate that, in select cases, three of the four blendstocks evaluated in our study could compete with Jet-A under the highest oil price scenario, but average MSPs will still be approximately twice that of Jet-A without further yield and process improvements.

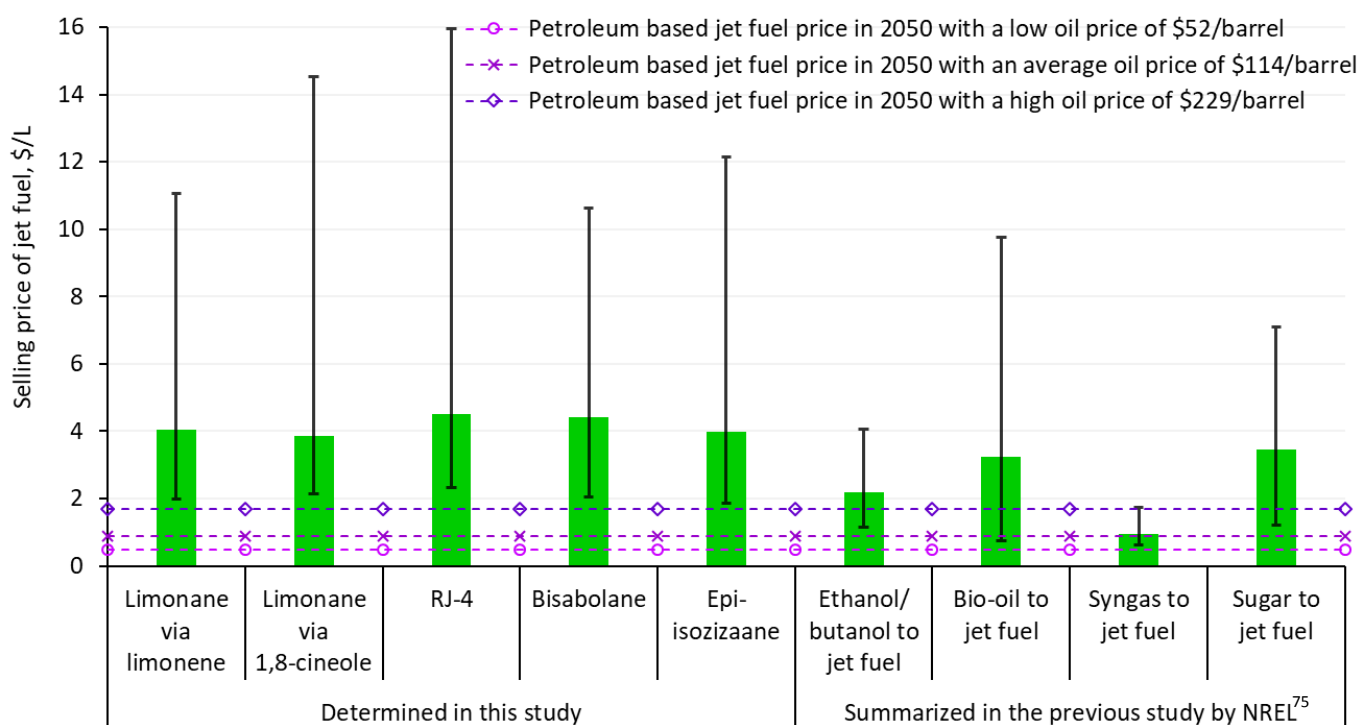


Fig. 4. Comparison of baseline-scenario bio-jet fuel prices in this study, prices from previous bio-jet fuel studies, and petroleum jet fuel prices based on three oil price scenarios (all 2018 U.S. dollars). The sensitivity bars for this study represent the range after running 5000 trials using probability distributions from the baseline scenario, and bars for other routes denote ranges of values from different studies summarized by NREL.<sup>75</sup> Projected petroleum jet fuel price based on the 2018 Annual Energy Outlook.<sup>76</sup> The NREL study<sup>75</sup> summarized results from several past analyses, normalized on the basis of feedstock cost, financial assumptions, and analysis methods (Notes and References §).

### 3.2 Minimum selling price sensitivity to different pathways, product yields, and ionic liquids

Efforts to reduce or eliminate some of the required process chemicals and utilities are essential to reducing the minimum selling price of bio-based jet fuel molecules. Our results suggest that switching to protic ILs and micro-aerobic bioconversion could reduce costs, although only modestly. Fig. 3 depicts the minimum selling price of jet fuel molecules with aerobic bioconversion pathways, [Ch][Lys] pretreatment, and three different product yields. Similar results with micro-aerobic pathways are provided in the ESI-S5, along with results reflecting a switch to ethanolamine acetate ([EOA][OAc] - a protic IL). Moving to a micro-aerobic bioconversion process requires less oxygen (vvm), a smaller reactor size, and ultimately consumes less electrical energy and cooling water when compared to aerobic bioconversion; this lowers the hydrolysis and bioconversion cost by 30% and reduces overall MSP by 10% assuming the same product yield for both bioconversion pathways. However, if a switch to micro-aerobic conditions significantly reduces product yields, quantifying the tradeoff will be crucial, as the product yield is the single most influential parameter to the MSP (Fig. 5).

Shifting from a [Ch][Lys] to a protic IL ([EOA][OAc]) poses similar tradeoffs. [EOA][OAc] is lower-cost, does not require pH adjustment before hydrolysis and bioconversion, and thus avoids regeneration step during IL recovery process, resulting in

a 57% lower pretreatment cost compared to using [Ch][Lys] (ESI-S5). However, the most recent experimental results suggest that [EOA][OAc] achieves lower sugar yields relative to [Ch][Lys], so the net savings are only 1-3% of the MSP (ESI-Table S2 and ESI-S5).

Regardless of individual pathway, micro vs. fully aerobic conditions, or IL choice, the MSPs begin to converge when product yields approach their theoretical maxima, indicating that much of the pathway-to-pathway variation in MSP stems from differing reported yields (as discussed earlier, yields of limonene, 1,8-cineole, linalool, bisabolane, and epi-isozizaane are 18.7%, 28.7%, 13.8%, 35.5%, and 22.2% of the stoichiometric maximum theoretical). However, it is unlikely that any of these routes will achieve >90% of theoretical yield in the near future, so it is crucial to explore the full array of process improvements that can be leveraged to approach or achieve the targeted selling price of jet fuel from biomass sorghum of \$0.66/L-Jet A (\$2.5/gal-Jet A).

### 3.3 Minimum selling price sensitivity to process parameters

The values of input parameters used in this study for the baseline scenario may vary with local conditions, the production scale, and at the time of commercial establishment. This is why the sensitivity bars in Fig. 3 and 4 show such a large range of possible MSPs. ESI-S7 presents several most influential parameters identified through a single-point sensitivity analysis. The two most important parameters are the yield of jet fuel

precursors from glucose and xylose, and the cellulose and hemicellulose content in the feedstock. Following these, other sensitive parameters are IL cost, loading rate and its recovery, sorghum biomass feedstock cost, capital investment, and sugar yield (glucose and xylose) during enzymatic hydrolysis. An efficient IL recovery process reduces makeup-IL resulting in the lower operating cost for IL. A reduction in the cost of process chemicals, biomass feedstock, and process equipment, unsurprisingly, reduce the annual operating cost and subsequently reduce the minimum selling price of jet fuel molecules.

To further explore a subset of important parameters, we conducted two-point sensitivity analysis comparing six variables against product yield, using limonane via limonene as a representative case, and holding all other parameters at their baseline values (Fig. 5). The most striking, although not surprising, improvements in MSP come from simultaneously increasing product yield from the simple sugars and the quality of biomass (determined by total carbohydrates). Selecting biomass with increased carbohydrates or engineering bioenergy crops to achieve this phenotype will improve the economics of the bio-jet fuel routes presented here, and any other biofuel/bioproduct derived from lignocellulosic sugars. Our results suggest that reaching at least 60% carbohydrates and a product yield from simple sugars of >30 wt% are required to produce limonene via limonene at <\$2/L-Jet A. Bioconversion time and the bioconversion reactor time are comparatively less influential than the others parameters. Also of note is that some of these relationships can be approximated as linear within the bounds of our analysis; this means that basic sensitivity analyses can be performed without the need to re-run full process simulations, in select cases.

### 3.4 Monte Carlo simulation results

Fig. 6 depicts the probabilistic results for the minimum selling price corresponding to each jet fuel molecule. Our analysis is meant to capture both epistemic uncertainty (limitations in

ascertainable knowledge) and aleatory uncertainty (natural unpredictability, often referred to as variability). Detailed uncertainties associated with each stage of the entire jet fuel production system are presented in the ESI-S8. Uncertainties associated with IL recovery and its cost are primarily epistemic, and result in pretreatment being the main driver of minimum selling price uncertainty. This is because the specific IL recovery process we model has not been demonstrated in the lab, and thus relies on literature data and simulated values. Biomass sorghum supply logistics are also associated with higher epistemic and aleatory uncertainty due to the large variation in feedstock harvest rate, moisture content, and feedstock collection area.

Improved field trial and yield modeling data can help reduce this uncertainty. Largely epistemic uncertainty associated with fermentable sugar yields, enzyme loading rate, bioconversion time, and utilities requirements drive the contribution of hydrolysis and bioconversion to minimum selling price uncertainty. Uncertainty associated with the amount lignin and biogas yielded from the unutilized fermentable sugars are the major drivers for the lignin utilization section. Compared to the other routes/molecules, bisabolane and limonane via 1,8-cineole have reduced spread because their currently-demonstrated yields are higher than for other intermediates, and current yields are treated as a lower bound in each case. Epi-isozizaane has reduced spread relative to limonane via limonene due to 18% higher current product yield and 13% higher energy density, although the lower boiling point of limonene constrains the expected range in energy demand for recovery. Full details are provided in ESI-S8.

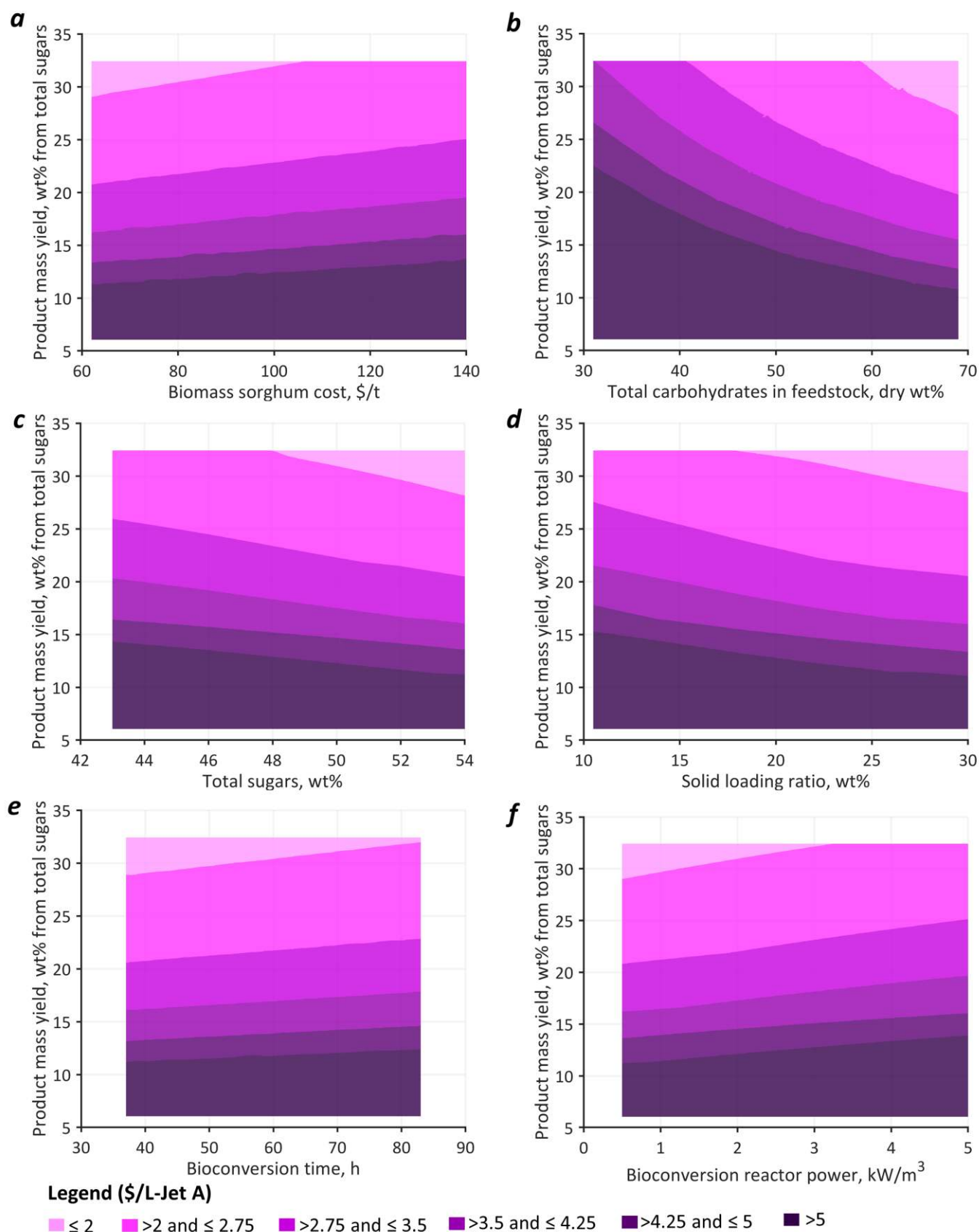


Fig. 5. Two-point sensitivity on the minimum selling price of limonane via limonene using the following combinations of parameters (a) limonene yield and biomass feedstock cost; (b) limonene yield and total carbohydrates of biomass; (c) limonene yield and total sugar yield from the feedstock; (d) limonene yield and solids loading during hydrolysis and bioconversion; (e) limonene yield and bioconversion time; and (f) limonene yield and bioconversion reactor power consumption.

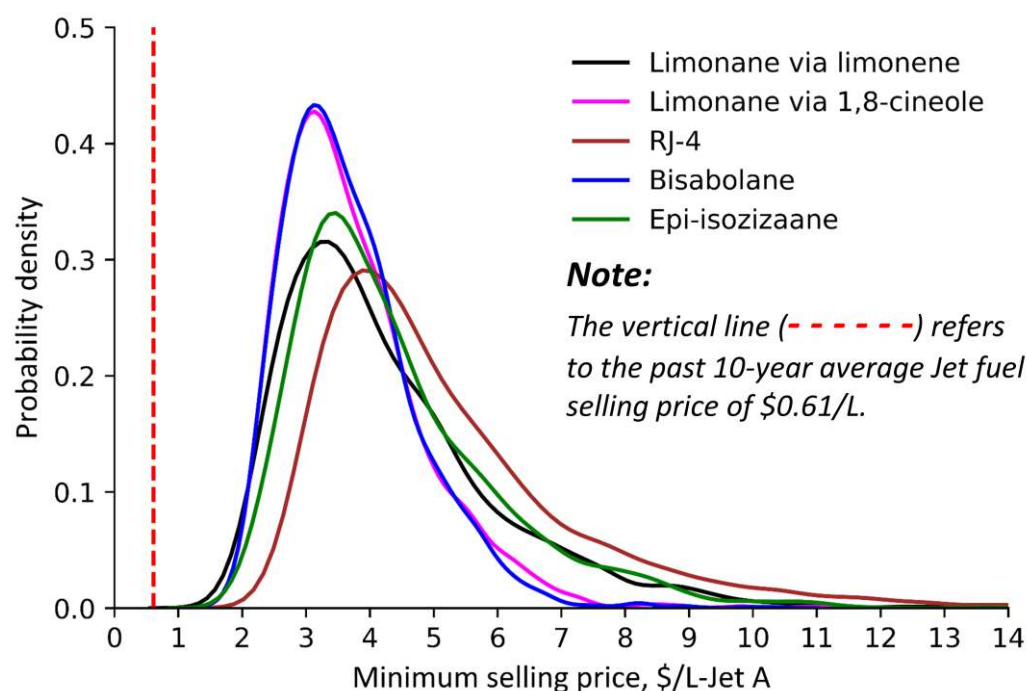


Fig. 6. Uncertainties associated with minimum selling price of different jet fuel molecules. Mean values correspond to the baseline input parameters (Table 1), varied based on their probability distributions, which are summarized in ESI-Table S2. The vertical dashed line (- - - -) denotes 10-year average jet fuel price at refineries of \$0.61/L.<sup>69</sup>

### 3.5 Future optimized selling price and roles for lignin valorization and carbon markets

While improvement in any single parameter (e.g., product yield, Fig. 4 and ESI-S5) is not sufficient to achieve the targeted MSP for the bio-jet fuel molecules routes analyzed here, a series of synergistic process optimization and intensification steps can be combined to approach the targeted price. ESI-S9 and S10 present step by step paths to reducing the MSP of each jet fuel molecule. A primary stepping-stone to reduce the minimum selling price is to increase the yield and productivity of jet fuel precursors. This could be achieved through metabolic engineering techniques and screening of potential hosts. We use 90% of the stoichiometric theoretical yield as an upper bound for each biologically-produced intermediate in the optimal case (ESI-S9). Biological production of ethanol, for example, reaches approximately 90% of stoichiometric theoretical yield. Host- and pathway-specific limitations for the jet fuel precursors studied here are likely to result in substantially lower maximum yields for these molecules, so 90% should be considered an absolute upper bound, but not necessarily feasible in the near or mid-term.

Another important avenue for cost reductions is improved biomass feedstock quality, through increased sugar content and decreased lignin (or modified lignin that lends itself to high-value products). The optimal composition of biomass sorghum considered in this study (Table 1) can be achieved with some photoperiod-sensitive or brown midrib (BMR) sorghum varieties.<sup>45</sup> The delivered cost of the sorghum, or any other biomass feedstock, can also be optimized. In our optimal case, we assume the biorefinery is located in a resource-rich area

(<40 miles of feedstock supply radius), thus reducing biorefinery gate costs to \$60/dry metric ton of sorghum. IL recovery and IL cost are important parameters to reduce the cost associated with pretreatment process. Previous studies<sup>38,51</sup> reported that 99% of IL recovery could be possible, along with a protic IL purchase cost of \$1/kg. We also project improvements in IL loading, achieving a minimum of 0.25 kg/kg-dry biomass.<sup>37</sup>

During hydrolysis and bioconversion, reaching 30 wt% solids loading reduces the required size of process equipment and the quantity of utilities for the downstream process. *E. coli* used to produce the selected jet fuel precursors is ideal as an aerobic microorganism. However, the bioconversion can be improved by using alternative microbes or strains of *E. coli* that can operate at micro-aerobic or close to anaerobic conditions. These collective efforts could reduce the minimum selling price of limonane via limonene, limonane via 1,8-cineole, RJ-4, bisabolane, and epi-isozizaane to \$0.77, \$0.91, \$1.33, \$0.83, and \$0.73 per L-Jet A, respectively. Further reducing the cost of RJ-4 requires improvements in its upgrading process (i.e. linalool to RJ-4), specifically by increasing turnover numbers (TONs), yields, and selectivity for the ruthenium catalysts at lower catalyst loading rates (Fig. 1). The progress in this area has been realized as the previous study<sup>77</sup> reported an improved catalyst TON and loading rate, although improvements specifically for RJ-4/intermediate products yields have not yet been demonstrated in the literature.



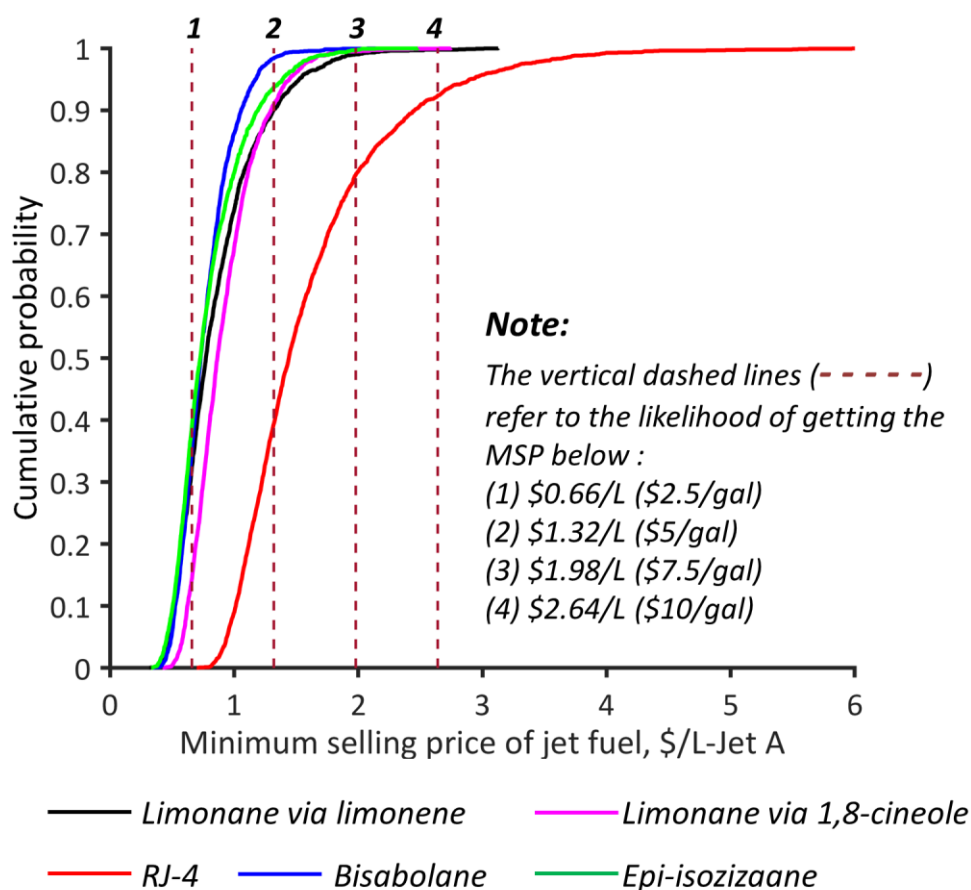


Fig. 7 Likelihood of reaching different target prices for each blendstock with potential future improvements (see ESI-S9)

The optimal prices reported in this study can be thought of as theoretical minima, with very little room for further improvement without major changes in process configuration. RJ-4 is a possible exception, as we have not modeled potential improvements in catalytic upgrading. Fig. 7 demonstrates the likelihood of reaching different target prices. Apart from RJ-4, there is a >85% probability of achieving prices below \$1.32/L (\$5/gal). Without improvements in the catalytic upgrading, the minimum selling price of RJ-4 has a 40% probability of reaching less than \$1.32/L (\$5/gal), and an 80% chance of selling for less than \$1.98/L (\$7.5/gal). Analogous results for GHG emissions are presented in the ESI-Figure S14. It is notable that the optimal prices are still higher than the targeted selling price of \$0.66/L-Jet A (\$2.50/gal-Jet A), although they are not far from the mid-range 2050 jet fuel price, if oil reaches \$114/barrel (2018 dollars)<sup>76</sup> (Fig. 4). In lieu of significant increases in oil prices, valuable co-products or policy supports will be necessary to be competitive in the fuel market.

This study considers two different means of further reducing the MSP to \$0.66/L-Jet A: 1) conversion of lignin to a high-value product and 2) a price paid for avoided GHG emissions relative to conventional Jet A. In the former case, lignin can no longer be used for on-site energy generation, so additional natural gas must be imported, along with grid electricity. As a proxy for a

hypothetical lignin upgrading unit, we use a previous TEA on fast pyrolysis of the lignin obtained from cellulosic biorefineries,<sup>78</sup> which corresponds to process equipment costing \$100M and 10 MW of electricity demand, including additional upgrading<sup>79</sup> to produce a valuable product. The yield of the lignin-derived co-product is assumed to be 25 wt%. Under these assumptions, the selling price of the lignin-derived co-product must be \$1.95, \$2.2, \$5.3, \$2.1 and \$1.9 per kg for limonene via limonene, limonene via 1,8-cineole, RJ-4, bisabolane, and epi-isozizaane, respectively, to hit the targeted selling price of \$0.66/L-Jet A (Fig. 8 and ESI-S10).

Alternatively, a policy support offering monetary GHG mitigation credits could enable bio-jet fuels to reach the targeted selling price. We calculate the values per metric ton CO<sub>2</sub> required to achieve the MSP target and compare with currently-active cap-and-trade markets and other official monetary values placed on GHG mitigation. We calculate this by dividing the net GHG emissions reduction per liter of Jet A equivalent by the cost premium per liter for each bio-jet fuel molecule. The net GHG emissions also account for the direct and indirect land use changes.<sup>40,80</sup> Further detail on input assumptions and data sources is provided in the ESI-S1.3.



Regardless of specific conversion pathway, the GHG footprints for bio-jet fuel molecules, including estimated direct and indirect land use change impacts, are higher than conventional Jet-A at currently-achievable yields. The bio-jet molecules reach near-parity with Jet-A when the yield is increased to 50% of theoretical (3 to 5% reduction for limonane via limonene and limonane via 1,8-cineole, and 1% to 4% greater than Jet-A for other molecules). This results in very high GHG mitigation costs (\$15861-\$25662 per metric ton-CO<sub>2</sub> avoided, where applicable). Maintaining 50% of theoretical yield, shifting to microaerobic conversion, and a protic IL reduces the GHG emissions mitigation cost to \$1814-\$4048 per metric ton-CO<sub>2</sub> avoided (still well above what could be considered justifiable). Increasing yields to the theoretical maxima reduces the GHG mitigation cost to \$454-850 per metric ton-CO<sub>2</sub> avoided. This is still far above any current market prices but closely represent a recently estimated social cost of carbon: \$177 to 805 per metric ton CO<sub>2</sub>.<sup>81</sup>

Optimal process conditions (considered 90% of the theoretical yield combined with additional process improvements discussed previously (ESI-S9)) reduce GHG emissions by 86-94% of the petroleum-based jet fuel, resulting GHG emissions mitigation costs that are an order of magnitude lower in most cases: \$45, \$85, \$217, \$58, and \$32 per metric ton-CO<sub>2</sub> avoided for limonane via limonene, limonane via 1,8-cineole, RJ-4, bisabolane, and epi-isozizaane, respectively. In addition to the process improvements, this reduction in GHG emissions owed to bioenergy sorghum's net soil organic carbon (SOC) sequestration potential (referred to as direct land use change impacts), owed to its high biomass yields and deep root systems.<sup>82</sup> However, the SOC gain with biomass sorghum farming in cropland/pasture land presented in the DOE Billion-Ton study<sup>82</sup> is based on only a limited number of counties, and is highly uncertain; further analysis is needed to better understand the net impact on emissions/sequestration. We accounted the variability present in data and presented sensitivity bars (Fig. 8).

The higher GHG emissions mitigation cost for RJ-4 is due to its higher production cost (Fig. 8) and additional material associated with oligomerization and hydrogenation process compared to other jet fuel molecules. Variations in GHG mitigation costs among the other bio-jet fuel molecules are owed to differences in the facility energy balances, which are important drivers of emissions but are less significant contributors to MSP. Our results suggest that the GHG mitigation cost for biomass-derived jet fuel estimated in the Schäfer et al. study<sup>83</sup> of \$10-70 per metric ton-CO<sub>2</sub>-avoided could be achieved with three of the five routes presented here under optimal process conditions (Fig. 8 and ESI-S9). For

comparison, the U.S. Environmental Protection Agency previously planned to value CO<sub>2</sub> avoidance at \$46/metric ton by 2020, while California's cap-and-trade CO<sub>2</sub> market reached a price of \$15.10/metric ton CO<sub>2e</sub> as of March 2018.<sup>84</sup> In the most recent Marginal Cost of Abatement (MAC) curve produced by McKinsey & Company, most carbon capture and storage (CCS) options for power plants or industrial facilities had estimated MACs of \$54-\$59/metric ton CO<sub>2e</sub> (2018 dollars).<sup>66</sup> Given that aviation fuel has been acknowledged as one of the most costly and challenging transportation sectors to significantly decarbonize, the mitigation costs corresponding to optimal conditions are fairly reasonable.

### 3.6 Use-phase advantages in commercial aviation

Although our results presented so far have been normalized on the basis of lower heating value (LHV) (see ESI-Table S1), airlines place additional value on very energy-dense fuels because of the potential aircraft range and efficiency advantages. Limonane and bisabolane both have calculated LHVs above Jet-A, and all four bio-jet molecules have higher density than Jet-A. Using these values and the Breguet range equation<sup>83,85</sup> (ESI-S3), we calculated the expected fuel cost savings for each bio-jet fuel if used as a 100% drop-in replacement for Jet-A (Fig. 9- a and b). This should be considered an upper bound, as aromaticity and lubricity of the final fuel will almost certainly limit the blending ratio. For context, a previous study<sup>88</sup> reported that the conventional jet fuel is comprised of, on average, aromatics (18 vol%), naphthenes (35 vol%), paraffins (45 vol%), and olefins (2 vol%). Further research is needed to determine optimal blending ratios. Our results show fuel savings assuming that the bio-jet molecules are available for the same price as Jet-A (a 2050 projection based on the high oil price scenario: \$1.68/L in 2018 dollars). Without a policy support or other means of reaching cost parity, of course, these savings would not be realized due to the higher MSP for bio-jet fuels.

Fig. 9 b depicts two case examples for fuel cost and GHG savings considering an international flight (San Francisco (SFO), USA to London (LHR), UK) and a domestic flight (San Francisco (SFO), USA to New York (JFK), USA). In this typical international flight, fuel cost in the range of \$17 to \$64 per passenger could be saved (out of a total per-passenger fuel cost of \$756 with the conventional jet fuel). About half of this fuel cost can be saved in the selected domestic flight (San Francisco to New York City). In this case, an airline will be willing to pay about 4-14 cents (in 2018 dollars) more per liter for the bio-jet fuel due to higher energy density. If fuel prices are lower, this price premium will decrease.

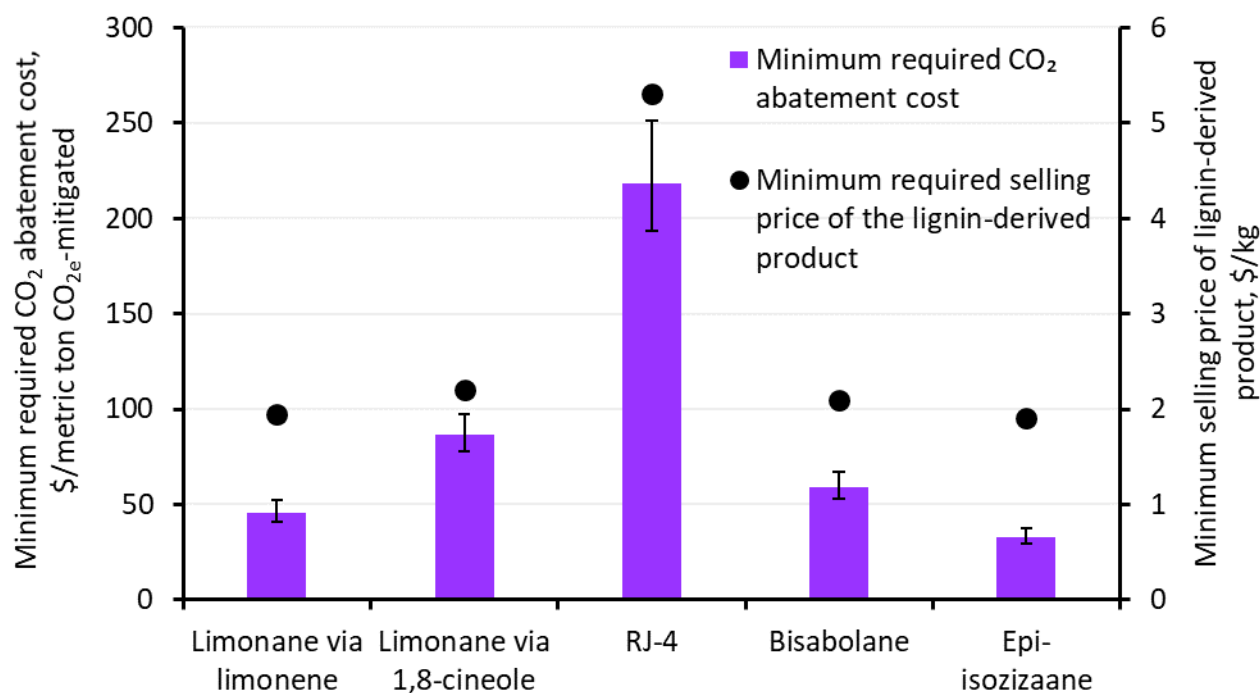


Fig. 8 Two options for reaching the \$0.66/L (\$2.50/gal) MFSP target in the 'Optimal' case (referring to process conditions outlined in ESI-S9): Deriving value from lignin and selling CO<sub>2e</sub> credits in a cap-and-trade marketplace. Bars and primary axis denote required minimum selling price of lignin-derived product. Black dots and secondary axis denote the minimum required price per metric ton of CO<sub>2e</sub> mitigation (for comparison, California cap-and-trade market price is \$15.10/metric ton CO<sub>2e</sub>).<sup>84</sup> The sensitivity bars represent uncertainty in GHG mitigation costs, including direct and indirect land use change.<sup>40,80,86,87</sup>

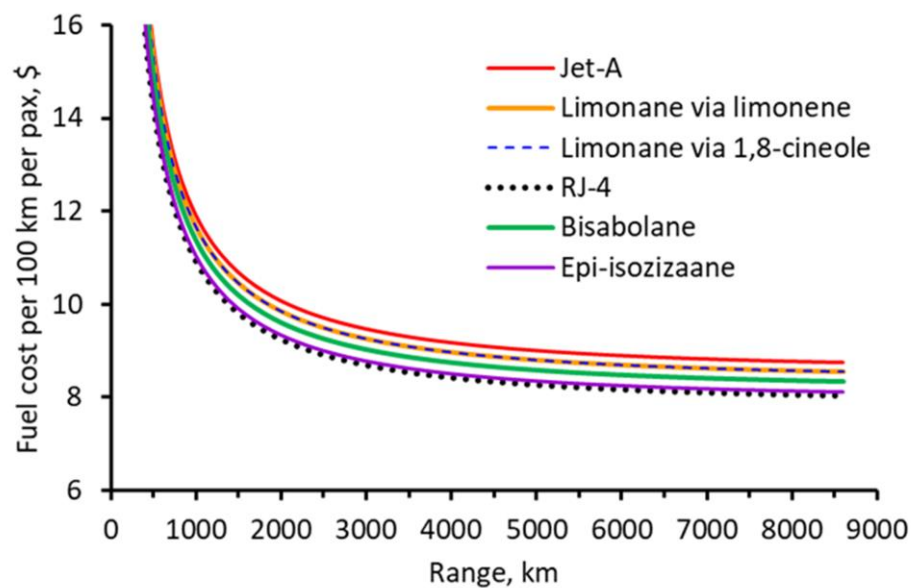
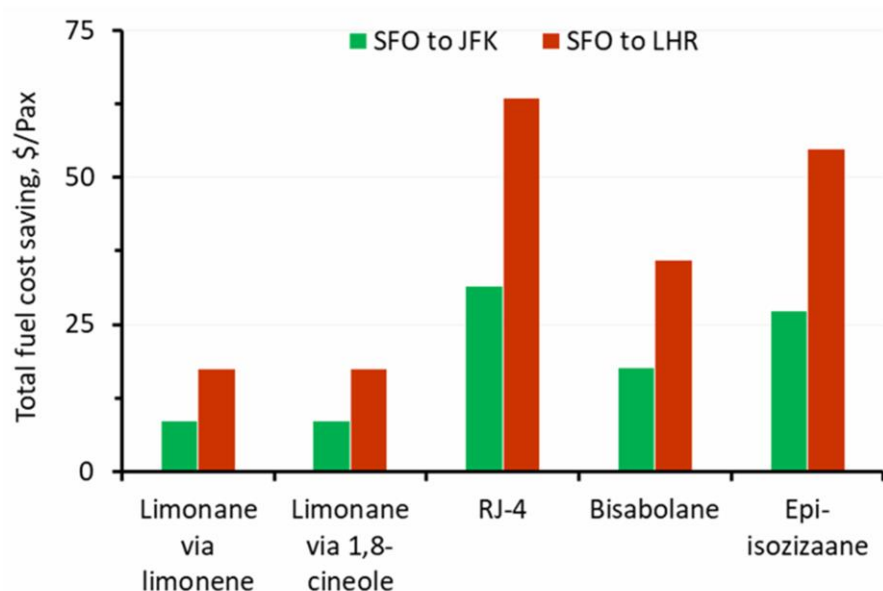
**a. Fuel cost over the range****b. Fuel cost saving in typical domestic and international flights**

Fig. 9 (a) Fuel cost across possible ranges per 100 km per passenger (pax) and (b) and fuel cost savings per passenger (pax) for typical domestic and international flights (all in 2018 U.S. dollars, assuming \$1.68/L fuel price for both bio-jet and Jet A). San Francisco (SFO), USA to New York (JFK), USA is estimated at 2247 nm or 4162 km and San Francisco (SFO), USA to London (LHR), UK is estimated at 4664 nm or 8638 km.<sup>83,85</sup> All the prices are in 2018 U.S. dollars.

## 4. Conclusions

In this study, we consider a promising biomass sorghum feedstock and evaluate the economic feasibility and greenhouse gas emissions mitigation costs of five different jet fuel molecules. We assess the contributions from each stage of the entire supply chain (integrating feedstock supply logistics and the downstream conversion processes) to the minimum selling price of the selected molecules and their probabilistic distributions results are presented. The results suggest that the yield of the targeted product and the quality of biomass feedstock determined by cellulose and hemicellulose are the primary drivers to achieving economic competitiveness and to reducing the greenhouse gas emissions mitigation cost. Additional efforts, including metabolic and process engineering and lignin valorization, are required to achieve the targeted minimum selling price of \$0.66/L-Jet A. The engineering of hydrogenation and /or oligomerization process is essential to improving jet fuel yield and selectivity with cheaper metal catalysts.

Process intensification, optimization, and near-theoretical yields for biologically-produced precursors can reduce the minimum selling prices from \$10.6, \$6.4, \$14.4, \$6.2, \$8.9 per L to \$0.77, \$0.91, \$1.33, \$0.82, and \$0.73 per L-Jet A for limonane via limonene, limonane via 1,8-cineole, RJ-4, bisabolane, and epi-isozizaane, respectively. Reaching the targeted price of \$0.66/L requires that lignin-derived products to be sold at a minimum of \$1.9/kg, which in itself requires improvements in lignin engineering and conversion to valuable bioproducts. However, even without lignin valorization, the optimal process conditions correspond to GHG mitigation costs within a reasonable range, particularly given the challenges associated with decarbonizing the aviation transportation sector, reaching a minimum of \$29/metric ton CO<sub>2e</sub> avoided. This result suggests that, while decarbonization of the aviation sector is challenging, future research can eventually produce jet fuels that are compatible with current engines and offer compelling environmental benefits at a fairly modest additional cost.

At the upper end of future fuel price scenarios, we find that airlines may also be willing to pay a premium for these bio-jet fuel molecules because of their higher volumetric energy density. This premium could be as high as 4–14 cents per liter when compared to petroleum-based jet fuel due to the higher energy density and if both fuels are available at the same price of \$1.68/L (2018 price) in the future. However, additional work to optimize promising metabolic pathways and reach near-theoretical yields is essential to achieving these goals. Future work should integrate metabolic models with technoeconomic analysis and life-cycle assessment to better understand and quantify the theoretical limits of specific routes and enable the selection of target molecules with the greatest potential to be commercialized.

## Conflicts of interest

There are no conflicts to declare.

## Acknowledgements

We thank Ben Harvey for his invaluable feedback, N.V.S.N. Murthy Konda for his contribution to early technoeconomic analysis models, and Seema Singh for leading the development of the integrated high-gravity process. We would also like to thank Harvey Blanch for laying the groundwork for this research. This work was part of the DOE Joint BioEnergy Institute (<http://www.jbei.org>) supported by the U.S. Department of Energy, Office of Science, Office of Biological and Environmental Research, through contract DE-AC02-05CH11231 between Lawrence Berkeley National Laboratory and the U.S. Department of Energy. The United States Government retains and the publisher, by accepting the article for publication, acknowledges that the United States Government retains a non-exclusive, paid-up, irrevocable, world-wide license to publish or reproduce the published form of this manuscript, or allow others to do so, for United States Government purposes.

## Notes and references

‡ Supporting information includes input data associated with process modeling, the required materials and energy, and detailed results of the minimum selling price for each production step.

§ The alcohol to jet fuel pathways considered ethanol, n-butanol, and iso-butanol from feedstocks including corn grain, corn stover, wood, straw, sugarcane, and switchgrass. Feedstocks considered in bio-oil results include plant oils, waste oils, algal oils, and pyrolysis oils (from corn stover and wood). Feedstocks for the syngas-to-jet fuel route include coal, corn stover, wood, vegetative, and household waste. Sugar-to-jet fuel includes fermentation of sugar derived from corn stover, sugarcane, wood, and wheat straw.

- 1 EIA, Jet fuel consumption, price, and expenditure estimates, US Energy Information Administration, Washington, DC, 2016.
- 2 Petroleum & Other Liquids, US Energy Information Administration, Washington, DC, 2016.
- 3 L. Rye, S. Blakey and C. W. Wilson, *Energy Environ. Sci.*, 2010, **3**, 17–27.
- 4 EPA, U.S. Transportation Sector Greenhouse Gas Emissions, US Environmental Protection Agency, 2017.
- 5 N. Armaroli and V. Balzani, *Energy Environ. Sci.*, 2011, **4**, 3193–3222.
- 6 G. Renouard-Vallet, M. Saballus, G. Schmithals, J. Schirmer, J. Kallo and K. A. Friedrich, *Energy Environ. Sci.*, 2010, **3**, 1458–1468.
- 7 N. Savage, *Nature*, 2011, **474**, S9.
- 8 M. J. Dunlop, Z. Y. Dossani, H. L. Szmids, H. C. Chu, T. S. Lee, J. D. Keasling, M. Z. Hadi and A. Mukhopadhyay, *Mol. Syst. Biol.*, 2011, **7**, 487.
- 9 C. J. Chuck and J. Donnelly, *Appl. Energy*, 2014, **118**, 83–91.
- 10 D. Mendez-Perez, J. Alonso-Gutierrez, Q. Hu, M. Molinas, E. E. K. Baidoo, G. Wang, L. J. G. Chan, P. D. Adams, C. J. Petzold and J. D. Keasling, *Biotechnol. Bioeng.*
- 11 R. D. Whitworth, 1990, U.S. Patent 4,915,707.
- 12 P. P. Peralta-Yahya, M. Ouellet, R. Chan, A. Mukhopadhyay, J. D. Keasling and T. S. Lee, *Nat. Commun.*, 2011, **2**, 483–

- 488.
- 13 R. M. Phelan, O. N. Sekurova, J. D. Keasling and S. B. Zotchev, *ACS Synth. Biol.*, 2015, **4**, 393–399.
- 14 T. Tian and T. S. Lee, DOI:10.1007/978-3-319-31421-1.
- 15 J. Alonso-Gutierrez, R. Chan, T. S. Batth, P. D. Adams, J. D. Keasling, C. J. Petzold and T. S. Lee, *Metab. Eng.*, 2013, **19**, 33–41.
- 16 A. Hiremath, M. Kannabiran and V. Rangaswamy, *N. Biotechnol.*, 2011, **28**, 19–23.
- 17 X. Chen, D.-J. Zhang, W.-T. Qi, S.-J. Gao, Z.-L. Xiu and P. Xu, *Appl. Microbiol. Biotechnol.*, 2003, **63**, 143–146.
- 18 M. T. Fernández-Sandoval, J. Galíndez-Mayer, C. L. Moss-Acosta, G. Gosset and A. Martínez, *J. Chem. Technol. Biotechnol.*, 2017, **92**, 981–989.
- 19 Y. Huang, Z. Li, K. Shimizu and Q. Ye, *Bioresour. Technol.*, 2013, **128**, 505–512.
- 20 V. Koppolu and V. K. R. Vasigala, *Microbiol. insights*, 2016, **9**, MBI-S10878.
- 21 P. Xu and M. A. G. Koffas, *Biofuels*, 2010, **1**, 493–504.
- 22 J. Hannon, A. Bakker, L. Lynd and C. Wyman, in *Annual Meeting of the American Institute of Chemical Engineers: Salt Lake City*, 2007.
- 23 C. T. Trinh, J. Li, H. W. Blanch and D. S. Clark, *Appl. Environ. Microbiol.*, 2011, **77**, 4894–4904.
- 24 X. Yang, T. Li, K. Tang, X. Zhou, M. Lu, W. L. Ounkham, S. M. Spain, B. J. Frost and H. Lin, *Green Chem.*, 2017, **19**, 3566–3573.
- 25 B. G. Harvey, 2016, U.S. Patent 9,493,717.
- 26 P. P. Peralta-Yahya, M. Ouellet, R. Chan, A. Mukhopadhyay, J. D. Keasling and T. S. Lee, *Nat. Commun.*, 2011, **2**, 483.
- 27 R. M. Phelan, O. N. Sekurova, J. D. Keasling and S. B. Zotchev, *ACS Synth. Biol.*, 2014, **4**, 393–399.
- 28 R. Li, W. K. W. Chou, J. A. Himmelberger, K. M. Litwin, G. G. Harris, D. E. Cane and D. W. Christianson, *Biochemistry*, 2014, **53**, 1155–1168.
- 29 INL, Idaho National Laboratory, 2014.
- 30 J. R. Hess and K. L. Kenney, *INL Tech. Rep.*
- 31 S. Sokhansanj, E. Webb and A. F. Turhollow Jr, Oak Ridge National Laboratory (ORNL), 2008.
- 32 A. Turhollow, *Biomass and Bioenergy*, 1994, **6**, 229–241.
- 33 A. Turhollow, E. Wilkerson, and S. Sokhansanj, Oak Ridge National Laboratory, Oak Ridge, TN, 2009.
- 34 D. Humbird, R. Davis, L. Tao, C. Kinchin, D. Hsu, A. Aden, P. Schoen, J. Lukas, B. Olthof and M. Worley, National Renewable Energy Laboratory (NREL), Golden, CO., 2011.
- 35 A. Aden, M. Ruth, K. Ibsen, J. Jechura, K. Neeves, J. Sheehan, B. Wallace, L. Montague, A. Slayton and J. Lukas, National Renewable Energy Lab., Golden, CO, USA, 2002.
- 36 R. Davis, L. Tao, E. C. D. Tan, M. J. Bidy, G. T. Beckham, C. Scarlata, J. Jacobson, K. Cafferty, J. Ross and J. Lukas, National Renewable Energy Laboratory (NREL), Golden, CO, USA, 2013.
- 37 F. Xu, J. Sun, N. M. Konda, J. Shi, T. Dutta, C. D. Scown, B. A. Simmons and S. Singh, *Energy Environ. Sci.*, 2016, **9**, 1042–1049.
- 38 J. Sun, N. M. Konda, R. Parthasarathi, T. Dutta, M. Valiev, F. Xu, B. A. Simmons and S. Singh, *Green Chem.*, 2017, **19**, 3152–3163.
- 39 B. Neupane, N. M. Konda, S. Singh, B. A. Simmons and C. D. Scown, *ACS Sustain. Chem. Eng.*, 2017, **5**, 10176–10185.
- 40 DOE, *U.S. Dep. Energy*, 2016, **1160**, 448–2172.
- 41 N. R. Baral, R. Davis, M. K. Mann, J. Engel-cox and T. H. Bradley, National Renewable Energy Lab., Golden, CO, USA, 2018.
- 42 S. C. Murray, W. L. Rooney, S. E. Mitchell, A. Sharma, P. E. Klein, J. E. Mullet and S. Kresovich, *Crop Sci.*, 2008, **48**, 2180.
- 43 Y. L. Zhao, A. Dolat, Y. Steinberger, X. Wang, A. Osman and G. H. Xie, *F. Crop. Res.*, 2009, **111**, 55–64.
- 44 B.-Z. Li, V. Balan, Y.-J. Yuan and B. E. Dale, *Bioresour. Technol.*, 2010, **101**, 1285–1292.
- 45 K. Theerarattananoon, X. Wu, S. Staggenborg, J. Propheter, R. Madl and D. Wang, *Trans. ASABE*, 2010, **53**, 509–525.
- 46 L. Wu, M. Arakane, M. Ike, M. Wada, T. Takai, M. Gau and K. Tokuyasu, *Bioresour. Technol.*, 2011, **102**, 4793–4799.
- 47 D. Y. Corredor, J. M. Salazar, K. L. Hohn, S. Bean, B. Bean and D. Wang, *Appl. Biochem. Biotechnol.*, 2009, **158**, 164.
- 48 M. Koradiya, S. Duggirala, D. Tipre and S. Dave, *Bioresour. Technol.*, 2016, **199**, 142–147.
- 49 N. Qureshi, S. Liu, S. Hughes, D. Palmquist, B. Dien and B. Saha, *BioEnergy Res.*, 2016, **9**, 1167–1179.
- 50 J. Alonso-Gutierrez, E.-M. Kim, T. S. Batth, N. Cho, Q. Hu, L. J. G. Chan, C. J. Petzold, N. J. Hillson, P. D. Adams and J. D. Keasling, *Metab. Eng.*, 2015, **28**, 123–133.
- 51 A. Brandt-Talbot, F. J. V Gschwend, P. S. Fennell, T. M. Lammens, B. Tan, J. Weale and J. P. Hallett, *Green Chem.*
- 52 A. Dutta, J. A. Schaidle, D. Humbird, F. G. Baddour and A. Sahir, *Top. Catal.*, 2016, **59**, 2–18.
- 53 H. Meyer, W. Minas and D. Schmidhalter, *Ind. Biotechnol.*, 2016, 1–53.
- 54 K. Atsonios, M. A. Kougioumtzis, K. D. Panopoulos and E. Kakaras, *Appl. Energy*, 2015, **138**, 346–366.
- 55 SuperPro Designer - User's Guide; Intelligen, Inc.: Scotch Plains, NJ, 2014.
- 56 X. Wang, Y. Nie, X. Zhang, S. Zhang and J. Li, *Desalination*, 2012, **285**, 205–212.
- 57 J. Sun, J. Shi, N. M. Konda, D. Campos, D. Liu, S. Nemser, J. Shamshina, T. Dutta, P. Berton and G. Gurau, *Biotechnol. Biofuels*, 2017, **10**, 154.
- 58 X. Yang, T. Li, K. Tang, X. Zhou, M. Lu, W. L. Ounkham, S. M. Spain, B. J. Frost and H. Lin, *Green Chem.*, 2017, **19**, 3566–3573.
- 59 H. R. Beller, T. S. Lee and L. Katz, *Nat. Prod. Rep.*, 2015, **32**, 1508–1526.
- 60 H. A. Meylemans, R. L. Quintana, B. R. Goldsmith and B. G. Harvey, *ChemSusChem*, 2011, **4**, 465–469.
- 61 J. A. Aaron, X. Lin, D. E. Cane and D. W. Christianson, *Biochemistry*, 2010, **49**, 1787–1797.
- 62 EIA, Electricity Monthly, US Energy Information Administration, Washington, DC, 2018.
- 63 BioMAT, Bioenergy Market Adjusting Tariff, 2015.
- 64 W. Wang, L. Tao, J. Markham, Y. Zhang, E. Tan, L. Batan, M. Bidy, W. Wang, L. Tao, Y. Zhang, E. Tan, E. Warner and M. Bidy, 2016, 98.
- 65 L. Gustavsson and R. Madlener, *Energy*, 2003, **28**, 1405–1425.
- 66 T. Nauclér and P.-A. Enkvist, *McKinsey Co.*
- 67 N. R. Baral, O. Kavvada, D. M. Perez, A. Mukhopadhyaya, T. S. Lee, B. A. Simmons, C. D. Scown, Nature Energy, 2018. Under review.
- 68 L. Weigand, S. Mostame, A. Brandt-Talbot, T. Welton and J. P. Hallett, *Faraday Discuss.*, 2017, **202**, 331–349.
- 69 EIA, U.S. Kerosene-Type Jet Fuel Wholesale/Resale Price by Refiners, US Energy Information Administration,

- Washington, DC, 2018.
- 70 K. Atsonios, M. A. Kougioumtzis, K. D. Panopoulos, and E. Kakaras, *Applied Energy*, 2015, **138**, 346–366.
- 71 S. De Jong, R. Hoefnagels, A. Faaij, R. Slade, R. Mawhood, and M. Junginger, *Biofuels Bioprod. Biorefin.*, 2015, **9**, 778–800.
- 72 M. Pearlson, C. Wollersheim, and J. Hileman, *Biofuels Bioprod. Biorefin.*, 2013, **7**, 89–96.
- 73 R. Davis, A. Aden, and P. T. Pienkos, *Applied Energy*, 2011, **88**, 3524–3531.
- 74 D. Klein-Marcuschamer, C. Turner, M. Allen, P. Gray, R. G. Dietzgen, P. M. Gresshoff, B. Hankamer, K. Heimann, P. T. Scott, E. Stephens, and R. Speight, *Biofuels Bioprod. Biorefin.*, 2013, **7**, 416–428.
- 75 W.-C. Wang, L. Tao, J. Markham, Y. Zhang, E. Tan, L. Batan, E. Warner and M. Bidy, National Renewable Energy Lab.(NREL), Golden, CO, USA, 2016.
- 76 U.S. Energy Information Administration, Office of Energy Analysis, U.S. Department of Energy, Washington, DC, 2018.
- 77 V. M. Marx, A. H. Sullivan, M. Melaimi, S. C. Virgil, B. K. Keitz, D. S. Weinberger, G. Bertrand and R. H. Grubbs, *Angew. Chemie Int. Ed.*, 2015, **54**, 1919–1923.
- 78 N. R. Baral and A. Shah, *Fuel Process. Technol.*, 2017, **166**, 59–68.
- 79 M. M. Wright, D. E. Daugaard, J. A. Satrio and R. C. Brown, *Fuel*, 2010, **89**, S2–S10.
- 80 F. Dou, J. P. Wight, L. T. Wilson, J. O. Storlien and F. M. Hons, *PLoS One*, 2014, **9**, e115598.
- 81 K. Ricke, L. Drouet, K. Caldeira and M. Tavoni, *Nat. Clim. Chang.*, 2018, 1.
- 82 DOE, *2016 Billion-Ton Report, Volume 2: Environmental Sustainability Effects of Select Scenarios from Volume 1*, 2016.
- 83 A. W. Schäfer, A. D. Evans, T. G. Reynolds and L. Dray, *Nat. Clim. Chang.*, 2016, **6**, 412.
- 84 Climate Policy Initiative, California Carbon Dashboard, 2018.
- 85 M. Burzlaff, Department of Automotive and Aeronautical Engineering, Hamburg University of Applied Science, 2017.
- 86 California Air Resources Board, Sacramento, CA, USA, 2018.
- 87 J. Fargione, J. Hill, D. Tilman, S. Polasky and P. Hawthorne, *Science*, 2008, **319**, 1235–1238.
- 88 T. Edwards, In38th AIAA/ASME/SAE/ASEE Joint Propulsion Conference & Exhibit 2002 Jul 7 (p. 3874).